THE REPUBLIC OF TURKEY

BAHCESEHIR UNIVERSITY

VOLTAGE STABILITY ANALYSIS OF GRID CONNECTED WIND FARMS: A CASE STUDY IN TRAKYA TRANSMISSION SYSTEM

Master's Thesis

OLCAY BUĞU BEKDİKHAN

ISTANBUL, 2014

THE REPUBLIC OF TURKEY

BAHCESEHIR UNIVERSITY

THE GRADUATE SCHOOL OF NATURAL AND APPLIED SCIENCES

M.S. ELECTRICAL AND ELECTRONICS ENGINEERING

VOLTAGE STABILITY ANALYSIS OF GRID CONNECTED WIND FARMS: A CASE STUDY IN TRAKYA TRANSMISSION SYSTEM

Master's Thesis

OLCAY BUĞU BEKDİKHAN

Supervisor: Prof. Dr. Emin Tacer

ISTANBUL, 2014

THE REPUBLIC OF TURKEY

BAHCESEHIR UNIVERSITY

THE GRADUATE SCHOOL OF NATURAL AND APPLIED SCIENCES

M.S. ELECTRICAL AND ELECTRONICS ENGINEERING

Name of the Thesis: Voltage Stability Analysis of Grid Connected Wind Farms: A Case Study in Trakya Transmission System

Name/Last Name of the Student: Olcay Buğu Bekdikhan

Date of Thesis Defense:

This thesis has been approved by the Graduate School of Natural and Applied Science.

……

Assoc. Prof. Dr. F. Tunç BOZBURA

Director

I certify that this thesis meets all requirements as a thesis for the degree of Master of Electrical and Electronics Engineering.

……

Assoc. Prof. Dr. Çiğdem EROĞLU

Program Coordinator

This is to certify that we have read this thesis and we find it fully adequate in scope, quality and content, as a thesis for degree of Master of Science.

Examination Committee Members	Signature
Prof. Dr. Emin TACER	……
Prof. Dr. Sadettin ÖZYAZICI	……
Assis. Prof. Dr. Görkem ÜÇTUĞ	……

ACKNOWLEDGEMENT

Firstly, I would like to thank to my supervisor Prof. Dr. Emin Tacer for his support and his belief in me.

Secondly, I would like to thank to Assist. Prof. Dr. Gürkan Soykan for his valuable advice and help.

Also, I thank to Ali Aktaş from Trakya Load Dispatching Center for his help and attention.

Finally, I would like to thank to my family especially my father and my mother. Without their support and encouragement, I cannot complete this thesis.

İstanbul, 2014 Olcay Buğu BEKDİKHAN

ÖZET

ŞEBEKE BAĞLANTILI RÜZGAR SANTRALLERİNİN GERİLİM KARARLILIĞI ANALİZİ: TRAKYA İLETİM SİSTEMİNİN İNCELENMESİ

Olcay Buğu Bekdikhan

Elektrik-Elektronik Mühendisliği

Tez Danışmanı: Prof. Dr. M. Emin Tacer

Ağustos 2014, Sayfa 77

Fosil kaynakların azalması ve enerji ihtiyacının artması yüzünden son yıllarda alternatif enerji kaynakları özellikle rüzgar enerjisi oldukça ilgi çekmeye başlamıştır. Ancak bu kaynaklar şebekeye bağlandığı zaman bazı güç kalitesi problemlerine sebep olmaktadır. Bu problemlerden en önemlisi gerilim kararlılığıdır. Gerilim kararlılığı problemlerinin çözülmesi için çalışmalar hala devam etmektedir.

Türkiye'de devlet teşviğiyle, son on yılda rüzgar enerjisi yatırımları oldukça artmıştır. Ancak rüzgar santrallerinin Türkiye'nin enterkonnekte elektrik sistemine bağlandığında sebep olduğu güç kalitesi problemleri ile ilgili çalışmalar yetersizdir. Bu tezde en önemli güç kalitesi problemi olan gerilim kararlılığı araştırılmıştır. İlk olarak statik ve dinamik gerilim kararlılığı analiz metotları incelenmiştir. Statik gerilim kararlılığı analizi için süregelen güç akışı yöntemi uygulanmıştır. Daha sonra dinamik analiz için zaman domeni benzetim çalışmaşarı incelenmiştir.

Bütün benzetim çalışmaları için bir MATLAB toolboxı olan PSAT kullanılmıştır. Benzetim çalışmaları ilk olarak IEEE 9 baralı test sistemine rüzgar bağlantılı ve rüzgar bağlantısız olarak uygulanmıştır. Daha sonra PSAT'ta Trakya İletim Sistemi oluşturulmuştur. Buna göre iki durum senaryosu gerçekleştirilmiştir. Bunlardan birinde orijinal Trakya İletim Sistemi kullanılmıştır. İkinci senaryoda ise orijinal sistemdeki bir konvensiyonel santral, çift beslemeli asenkron generatörlü (DFIG) bir rüzgar santrali ile değiştirilmiştir. Süregelen güç akışı yöntemi kullanılarak iki durum içinde sistemin maksimum yüklenebilirlik limiti bulunmuştur. Rüzgar santrali bağlantısının maksimum yüklenebilirliği düşürdüğü görülmüştür. Daha sonra iki senaryo içinde sistemin arıza sonrası davranışı zaman domeni analizi ile incelenmiştir. Rüzgar santralinin arıza sonrasında daha iyi sonuç verdiği görülmektedir. Ayrıca, FACTS cihazlarının etkileri dinamik analiz ile bulunmuştur.

Anahtar kelimeler: Statik Gerilim Kararlılığı, Dinamik Gerilim Kararlılığı, Rüzgar Santralleri, PSAT

ABSTRACT

VOLTAGE STABILITY ANALYSIS OF GRID CONNECTED WIND FARMS: A CASE STUDY IN TRAKYA TRANSMISSION SYSTEM

Olcay Buğu Bekdikhan

Electrical & Electronics Engineering

Thesis Supervisor: Prof. Dr. M. Emin Tacer

August 2014, Pages 77

Alternative energy resources especially wind energy becomes popular in recent years because of decrement in fossil fuels and increasing energy demand. However, these sources cause some power quality problems when they are connected to grid. One of the most important problems is voltage stability. Nowadays, lots of studies are still continuing for solving this.

In Turkey, with incentive of government, wind energy investments highly increase in last decade. However, studies about power quality problems of wind farms for Turkish electricity system are insufficient. In this thesis, voltage stability which is the most important power quality problem was investigated. Firstly, static and dynamic voltage stability analyzing methods were examined. Continuation power flow method for static voltage stability analysis was applied. Then, time domain simulations were investigated for dynamic analysis.

In order to achieve all simulations, PSAT which is a MATLAB toolbox was used. Firstly, simulations were completed on IEEE 9 bus test system with and without a wind farm connection. Then, Trakya Transmission System was created in PSAT. Two cases were composed. One of them is the original Trakya Transmission System. In the second case, one conventional power plant is changed with a DFIG based wind farm. Maximum loadability limits of both cases were found with continuation power flow method. It was obtained that wind farm connection decrease the loadability limit. After this, fault ride through (FRT) capability of both cases were investigated with time domain simulations and it was found that wind farm connection increase the FRT capability of the system. Wind farms give better results after a three phase fault. Also, effects of FACTS devices were obtained with the dynamic analysis.

Key words: Static Voltage Stability, Dynamic Voltage Stability, Wind Farms, PSAT

TABLE OF CONTENTS

LIST OF TABLES

LIST OF FIGURES

LIST OF ABBREVIATIONS

AC	:	Alternating Current
CPF	:	Continuation Power Flow
DAE	:	Differential Algebraic Equation
DC	:	Direct Current
DFIG	:	Doubly-Fed Induction Generator
EESG	:	Electrically Excited Synchronous Generator
FACTS	:	Flexible Alternating Current Transmission Systems
FC-TCR	:	Fixed Capacitor with Thyristor Controlled Reactor
GHG	:	Greenhouse Gases
HVDC	:	High Voltage Direct Current
IEEE	:	The Institute of Electrical and Electronics Engineers
PM	:	Permanent Magnet
PMSG	:	Permanent Magnet Synchronous Generator
PSAT	:	Power System Analysis Toolbox
SCIG	:	Squirrel Cage Induction Generator
STATCOM	:	Static Synchronous Compensator
SVC	:	Static Var Compensator
TCSVC	:	Thyristor Controlled Static Var Compnsator
TSCS	:	Thyristor Controlled Series Compensator
TSC-TCR	:	Thyristor Switched Capacitor- Thyristor Controlled Reactor
UPFC	:	Unified Power Flow Controller
WSCC	:	Western System Coordinating Council

LIST OF SYMBOLS

Mass	: m
Velocity	: V
Powe	: P
Air Density	: ρ
Swept Area	: A
Power Coefficient	: C_p
Voltage	: v
Resistance	: R
Current	: i
Flux Linkage	: φ
Inductance	: L
Self Inductance	: L_s
Magnetizing Inductance	: L_m
Rotor Position	: θ
Park Transformation Matrix	: $[P]$
Angular Velocity	: ω
Electrical Torque	: T_e
Mechanical Torque	: T_m
Moment of Inertia	: J
System's Load Change	: λ
Bus Generation Active Power	: P_G
Bus Load Active Power	: P_L
Bus Injection Active Power	: P_T
Bus Generation Reactive Power	: Q_G

Bus Load Reactive Power : Q_L

Bus Injection Reactive Power : Q_T

Multiplier which specify load change rate at bus i while λ is changing : k_{Li}

Apparent power for calculating proper λ value : $S_{\Delta base}$

Constant which determines rate of generation change while λ is varying : k_{Gi}

Bus voltage angles' vector : $\underline{\delta}$

Bus voltage magnitudes' vector : $\underline{V}$

Tangent vector : t

A row vector which k^{th} element is one and the others are zero : $\underline{e_k}$

State Variables : x

1. INTRODUCTION

1.1 BACKGROUND

Energy demand of the world was met by only fossil fuels in last centuries. In old times, fossil fuels were enough because industry was not developed. However, with technological development, growing industry and increasing population, energy demand was increased day by day. Fossil fuels which take many years for arising become insufficient. Besides their depletion, these fuels cause environmental pollution. They are burned while producing electricity. Therefore, lots of harmful gases especially carbon dioxide spread. These gases which also named as greenhouse gases (GHG) increase the temperature of world. Thus they cause climate change and global warming. As a result of these situations, human tend to renewable energy sources such as wind, solar, geothermal and etc. First studies were achieved by using water (Shafiullah and others 2013). However, in last decades, other renewable sources also took attention. Wind energy is the fastest growing one. Lots of investments are made and news are planning. In 2000, total capacity of wind plants was detected as 17400 MW. This increases to 237669 MW in 2011. It is supposed to increase more. In figure 1.1, installed wind energy capacity cumulative distributions by years can be seen (Shafiullah and others 2013).

Figure 1.1: Installed wind energy capacity of world

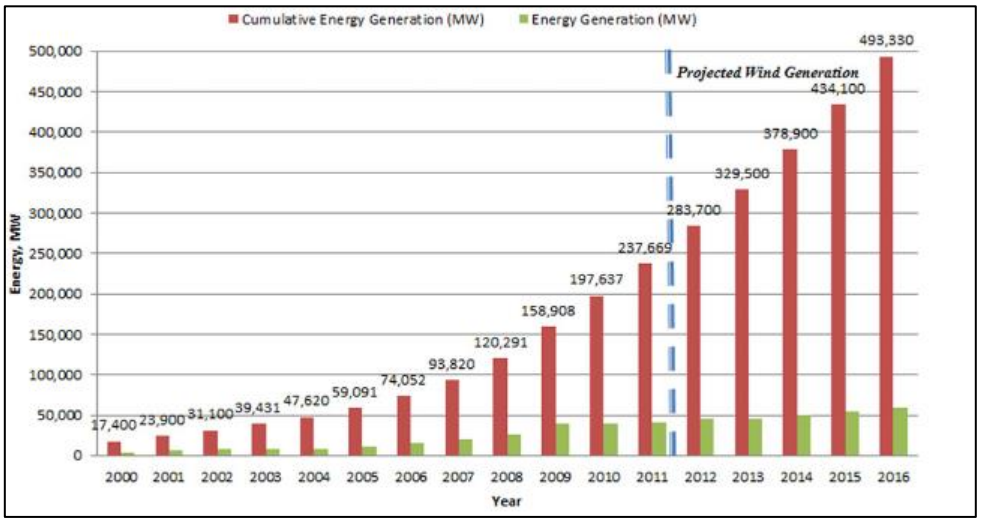

Reference: (Shafiullah and others 2013)

Besides their advantages, growing wind energy carries some problems with it. The main reason of it is intermittent nature of wind. Wind cannot be predicted certainly. Therefore, balance problem between production and consumption occurs. As a result of this, voltage problems such as voltage swell, dips and sags came out. The most important problem is voltage collapse because it takes long time to be fixed. In order to avoid these, lots of studies about grid integration of wind farm were completed. Some of them can be seen in (Chen 2005), (Bhumkittipich and Jan-Ngurn 2013) and (Xiaodong and others 2010). Voltage stability assessments of wind farms are still a popular subject. There are lots of analyzing methods and new solutions are developed day after day. However, continuation power flow is the most common voltage stability analysis method and it is preferred in this thesis.

1.2 MOTIVATION

In Turkey, energy demand is still met by fossil fuels or electricity which is exported. However, renewable energy starts to become popular in Turkey too. Government gives incentives for renewable energy. Because of this, investments in the energy are increased nowadays. Wind energy is mostly preferred renewable source by investors. Figure 1.2 includes cumulative distribution of installed wind capacity in Turkey in years (TUREB 2014). As it can be seen, wind plant capacity increases in recent years.

Figure 1.2: Cumulative distribution of installed wind plants in Turkey for years

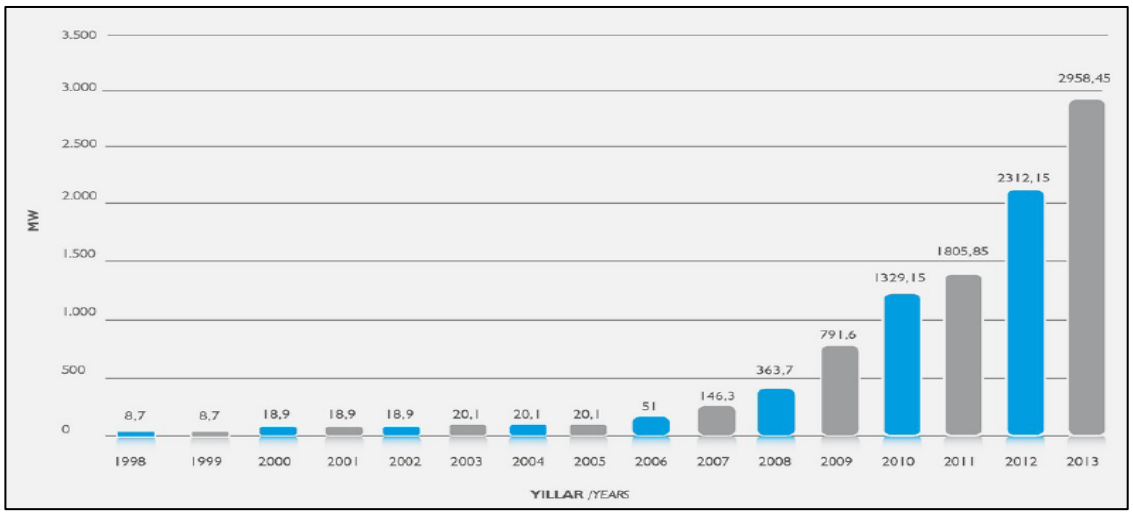

Reference: (TUREB 2014)

Like in the other countries, this increment will bring voltage stability problems. According to investments, wind power plant installation will more increase in future

years. However, there are few researches for voltage stability assessment of wind plants in Turkish electricity system. In (Keskin 2007), voltage stability is examined for a Turkish system without a wind farm. Also, in the study (Guleryuz 2010), Bursa Transmission system is examined for static voltage stability. In this thesis, wind farms are compared with conventional power plants and both dynamic and static voltage stability analyzes had been achieved.

1.3 OBJECTIVE OF THESIS

The main objective of this thesis is detecting voltage stability effects of grid connected wind farms. Also, another aim is comparing effects of conventional power plants and wind farms when they are connected to grid. Trakya region was chosen as case study. Both static and dynamic voltage stability analyzes will be achieved for this region.

1.4 SCOPE OF THESIS

The scope of this master thesis is investigating effects of wind farms on voltage stability. For this purpose static and dynamic voltage stability assessment will be applied to Trakya transmission system. For the static analyzes, continuation power flow method will be achieved for different cases. Effects of wind farms and conventional power plants on static voltage stability will be compared. For the dynamic analyzes, time domain simulation will be done. Then, a three phase fault will be applied and system behavior after the fault will be examined with and without wind farm connection. Also, in order to improving stability, FACTS devices will be investigated.

1.5 THESIS ORGANIZATION

Thesis consists of nine sections. The first section is the introduction. In the second section literature review is represented. In literature review, previous studies are clarified and difference and reform of this thesis are explained. After, common wind turbine technologies are explained in third section. Then, mathematical model of DFIG which is selected for this project is represented in fourth section. In Section 5, voltage stability is investigated. Then, static voltage stability analysis and dynamic voltage stability analysis are explained respectively in section 6 and section 7. In section 8, reactive power compensation's effects on voltage stability are represented. FACTS devices which are used in the thesis are explained and mathematical models of it is given. Then, in section 9, simulation program PSAT and reliability test of it are represented. After that, Trakya Transmission System is examined as a case study in

section 10. Continuation power flow and time domain results of the case study are given. All results and commends are represented as conclusion in section 11.

2. LITERATURE REVIEW

Depletion in the fossil fuels, increasing population and rising energy demand cause tendency to renewable energy resources. As a result of this, wind power plant installation increase day by day. However, wind is an intermittent source. Production time and amount cannot be detected certainly. This situation cause important power quality problems especially voltage stability. When voltage instability occurs, voltage collapse can be happened and sustainability of electricity cannot be supplied. Repairing of the system takes long times. Therefore, voltage stability analysis of wind power plants should be achieved properly. This analysis should be completed statically and dynamically. With the tendency to wind energy, stability studies become more attractive.

In the literature, lots of studies were completed about voltage stability effects of wind farms. In the study of Aly, M.M. and Abdel-Akher, M. (2011) effects of wind power integration to a radial distribution system were investigated. Radial system includes 37 buses. In the paper, firstly, static voltage stability assessment methods were examined. Continuation power flow method was explained detailed. Then, continuation power flow process applied to radial distribution system and the weakest bus was detected according to maximum loadability results. After the detection, DFIG wind turbines were connected to the weakest bus and their power were increased gradually. At all power level, continuation power flow method was applied. It was concluded that increasing wind power penetration increase the maximum loadability of the system. Also effects of wind turbine's power factor were investigated. As a result of this, leading power factor was found as best choice. However, in this study, voltage stability was examined as only statically. There is no dynamic voltage stability assessment.

In another study of Zeng, Z. and others (2009) voltage stability effects of wind farms were investigated with and without reactive power compensation devices. IEEE 14 bus test system was used for simulations. Firstly, maximum loadability limit of the original system without reactive power compensation devices was found by hopf. bifurcation analysis. This analysis was completed under normal and contingency operation. Then, system was modified and wind penetration was supplied. Again, hopf bifurcation

method was applied and it was found that wind farm connection decrease maximum loadability of the system. After that wind farm was operated with SVC and capacitor banks. Then, static voltage stability analysis was found by hopf bifurcation method. As a result of this, it was found that wind farm with SVC gives higher loadability limit when it is compared with wind farm with capacitor banks. In this paper, effects of SVC and capacitor banks are obtained but again only static voltage stability analysis is completed.

(Khattara, A. and others (2013) investigated fault through capability of a grid connected DFIG. In order to achieve this, dynamic voltage stability analysis is applied. Two scenarios were created. First of it is DFIG connection to a transmission line and the other is DFIG connection to a distribution line. A simple system which includes 5 bus, 1 generator, 2 transformers and 2 lines were simulated in PSAT. Then, for each case, fault ride through capabilities after a 3 phase fault were found. In first case, DFIG was connected to transmission network. In the second case, DFIG was connected to a distribution network. In both cases, voltages of all buses were examined at before, during and after fault situations. In conclusion, it was found that when wind farm is connected to distribution network, it has a fault ride through capability. Voltage level can reach old value after the fault cleared. However, when wind farm is connected to a transmission network, voltage level cannot reach old value. Fault ride through capability of wind farm becomes insufficient. In this study, fault ride through capacity of wind farm is compared for transmission and distribution network for a simple fictive system. Only time domain simulations are used. Static analysis is not applied.

PEA distribution system of Thailand in terms of voltage stability was examined (Bhumkittipich, K. and Jan-Ngurn, C., 2013). Effects of new wind power plant installation were investigated. Before and after a wind farm connection, voltage stability of PEA was analyzed. In order to do this, continuation power flow method was applied. MATLAB toolbox PSAT was used for simulations. As a result of CPF, maximum loading point was found. Also, voltage magnitudes and phase angles of all buses were calculated. Before and after wind turbine connections situations, these values were compared. In conclusion, it was found that wind power plant installation decrease

maximum loadability limit. In this study only power flow and continuation power flow techniques are used. Dynamic analysis or effects of reactive power compensation are no investigated.

Dynamic stability analysis of DFIG based wind farm was completed (Abdelhalim, H.M. and others 2013). IEEE 14 bus test system is used for simulations. A wind farm is added to IEEE 14 bus test system's different buses and cases are created. Also, effects of wind farm connection point were obtained. Time domain simulation method was used for analysis. In this study, static voltage stability analysis is not applied. As a result of the simulations, it was concluded that wind farm connection through additional transmission lines contributes transient stability.

Guleryuz, M. (2010) examined the voltage stability effects of FACTS devices and wind farms. Firstly, IEEE 14 bus test system was used for simulations. Effects of different FACTS devices (SVC, TSCS, STATCOM) were investigated on test system. Then, Bursa transmission system was examined. Static voltage stability analysis was completed by continuation power flow method and maximum loadability limit was found. Then, effects of three different FACTS devices on loadability limit were compared. It was concluded that STATCOM supply highest loadability limit when it compares with others. After this, new wind farm installation was added the system. It was assumed that STATCOM is used with wind farm. Then, dynamic simulations were completed for contingency conditions and different STATCOM parameters' effects were obtained.

Canizares, C. and Munoz, J. (2012) made a comparison between wind farms and conventional power plants. IEEE 14 bus test system was used for simulations. Three different scenarios were created. One of them is original IEEE system. In the second, one of the synchronous generators was changed with unity power factor DFIG. In the final one, synchronous generator was changed with DFIG with terminal voltage control. For all cases, static voltage stability analysis was completed by continuation power flow method. It was concluded that highest loadability limit was obtained in original case.

Then for different wind power penetration level, dynamic analysis was achieved. It was found that higher wind power penetration level contributes system voltage stability.

In this thesis, both static and dynamic analyzes of wind farms were completed. For all simulations, PSAT which is a MATLAB toolbox is used. Firstly, in order to prove reliability of the PSAT, IEEE 9 bus test system was used. After this, Turkish electricity system was examined. Trakya transmission system was selected and data were obtained from Trakya Load Dispatching Center. In this study, three cases were created. One of them is original Trakya transmission system. In second case, one synchronous generator was changed with a DFIG based wind farm. Thus, comparison of wind farm and conventional power plants can be achieved. In the third case, an additional wind farm was connected to the system. For all cases, static voltage stability analysis was done. In the study of Guleryuz, static voltage stability analysis of wind farms is not examined. Also, in the study of Canizares only comparison of wind farm and conventional power plant was completed for IEEE test case. In this thesis, a real electricity system was analyzed. Comparison of DFIG based wind farm and conventional power plants was completed for this real system and static voltage stability analysis was completed. Also, static analysis was done for an additional wind farm to real case. Also, in Guleryuz's study, FACTS devices are examined for just statically. However, in this thesis, as distinct from Guleryuz's study, dynamic analysis of FACTS devices and wind farms were done. Comparison of DFIG and synchronous generator were completed dynamically. Also, as distinct from Canizares and Guleryuz's studies, fault ride through capability of system was found after a three phase fault. Effects of different FACTS devices on system behavior after a fault were obtained.

3. WIND TURBINE GENERATOR TYPES

Wind turbines can be classified as lots of different ways. According to generator types, three common wind turbines are preferred in studies. These are squirrel cage induction generator, permanent magnet synchronous generator and doubly fed induction generator. Features, advantages and disadvantages of these types are represented in following.

3.1 SQUIRREL-CAGE INDUCTION GENERATOR

One of the common wind turbine generators is squirrel cage induction generator (SCIG). In Figure 3.1, structure of this type wind turbine is illustrated. These wind turbines operate with a fixed or nearly fixed wind speed. This situation has both advantages and disadvantages. The disadvantage is gearbox usage. Squirrel cage wind turbines have to operate with a gearbox. However, gearbox has a high cost and space of it in the nacelle is large. This is the one of the disadvantages. The main disadvantage is reactive power consumption. Squirrel cage induction generators consume reactive power from grid. This is harmful for especially weak grids. In order to prevent this, generally capacitor banks are connected to generator in parallel.

Besides the disadvantages, there are also some advantages. Squirrel cage induction generators are simple, robust and inexpensive. Besides structural advantages, there are operational advantages too. These wind turbines operate with a fixed speed. Therefore, they can be connected to the grid directly. Thus, frequency control is achieved without using additional power electronic devices (Li and Chen 2008, Camm and others 2009).

Figure 3.1: Configuration of a wind turbine with squirrel cage induction generator

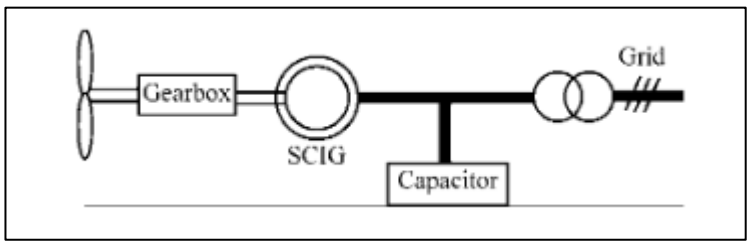

Reference: Li, H. and Chen, Z., 2008

3.2 PERMANENT MAGNET SYNCHRONOUS GENERATOR

Synchronous generators became more popular than SCIG in the last decade. The main reason of it is high torque at the low speeds. Also, these turbines are direct drive. A gearbox is not needed. Thus, gearbox cost is eliminated. However, these generators separate two different types; electrically excited synchronous generator (EESG) and permanent magnet synchronous generator (PMSG). Firstly, manufacturers tended to electrically excited synchronous generator and many wind turbines with EESGs were produced. Then, permanent magnet synchronous generator became more attractive because they remove excitation losses (Polinder and others 2005). Nowadays, most of synchronous generator wind turbines are produced with permanent magnets.

PMSGs can be used as direct drive or they can operate with a full scale power converter. Both of them operate with variable speed. In direct drive PMSG, there is no a gearbox. This is the main advantage of it because cost of gearbox is eliminated and also weight of it is removed. In addition, these generators are more reliable because there are less mechanical components than the others. However, because of gearbox's absence, generator operates with low speed so cost of generator is higher than geared PMSG. Also, a frequency converter should be used before grid connection (Li and Chen 2008). The basic configuration of direct drive PMSG is illustrated in Fig. 3.2.

Figure 3.2: Scheme of a direct drive PMSG wind turbine system

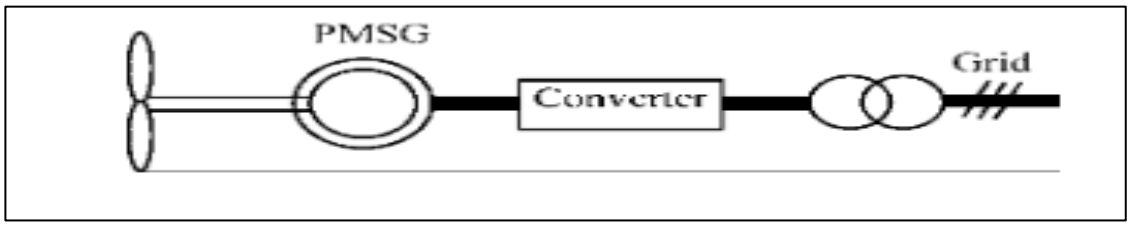

Reference: Li, H. and Chen, Z., 2008

PMSGs are also used with a gearbox. Nowadays, geared PMSG with full-scale power converter becomes more popular than the direct drive PMSG. In direct drive PM technology, generator operates with low speed because gearbox is removed. Unlike them, in order to get high speeds, single stage gearbox is used in geared PMSG. This is the main reason of increasing popularity. Even single stage gearbox has some disadvantages too, it is better than the other gearbox types because less mechanical

components are used. Also this type is efficient and robust too. However, power electronic converters should be used and this increase losses (Li and Chen 2008). A simple scheme of geared PMSG is given in Fig. 3.3.

Figure 3.3: Basic configuration of PMSG with a single stage gearbox

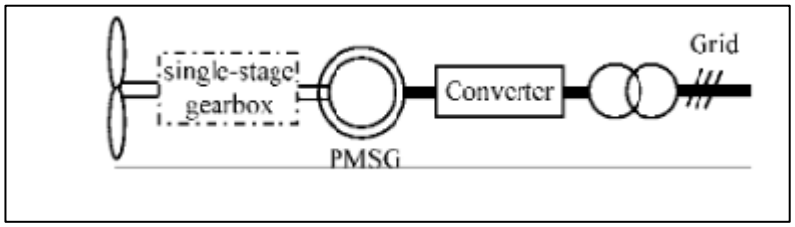

Reference: Li, H. and Chen, Z., 2008

3.3 DOUBLY-FED INDUCTION GENERATOR

In recent years, for wind turbine application, doubly-fed induction generators (DFIG) become more attractive. The main reason behind it, DFIG's can operate under wide range variable wind speed. A gearbox and a back to back converter are included in the basic structure of these wind turbines. They are called as DFIG because both of stator and rotor windings are connected to the grid. However, since stator is directly connected to the grid, rotor of DFIG is connected to a back to back converter via slip rings and then to the grid. Thus, when speed of the generator is higher than the synchronous speed, direction of the power transfer is from stator to the grid. If speed of the generator is below the synchronous speed, power is consumed from the grid (Camm and others 2009). This concept can be seen clearly in the Fig. 3.4.

Figure 3.4: DFIG based wind turbine configuration

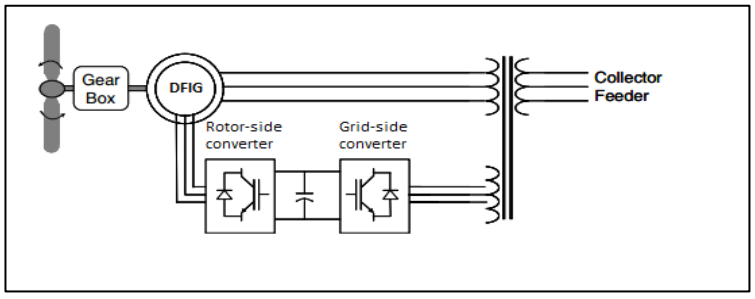

Reference: Camm and others 2009.

Controlling active and reactive power separately is a major advantage of DFIG's besides operating under wide range wind speed. Reactive power can be controlled with

grid side converter thus it isn't depending on the operation of generator. This situation is increase the performance (Li and Chen 2008).

There are also some disadvantages of the DFIG. Structure of it is more complicated than the other applications. For example, a lot of mechanical components are included. One of them is gearbox. In DFIG, multi-stage gearbox is used so cost and the weight of the turbine is increase. Also, it cause heating and noise. The other significant mechanical component is slip ring. It should be maintained regularly. In addition, at the fault condition, control strategies can be more complex than the other types (Li and Chen 2008).

4. MATHEMATICAL MODELS OF WIND TURBINES

In all wind turbine applications, kinetic energy of the wind is converted. Kinetic energy is converted to the mechanical energy in turbine blades and then this mechanical energy is converted to the electrical energy in wind turbine generator. In this thesis, voltage stability analysis of electricity which is produced from wind will be achieved. Therefore, for analyzing a DFIG based wind farm, firstly mathematical model of it should be established.

4.1 AERODYNAMIC MODEL

First energy conversion in wind turbine technologies is kinetic energy to mechanical energy. Wind comes to the turbine blades with a speed and blades start to rotate. Then, movement of blades turns the rotor and mechanical energy is obtained. This conversion is same for all different wind turbine types. The kinetic energy of air can be calculated from:

$$\text{Kinetic Energy} = \frac{1}{2}mV^2 \tag{4.1}$$

Also, power of the air is flow rate of kinetic energy per second and it can be extracted from 4.1 as:

$$\text{P} = \frac{1}{2}(\text{mass flow rate per second})V^2 \tag{4.2}$$

However, speed of upstream wind which is at entrance on the blades and speed of downstream wind which is at behind the blades are not equal. Therefore, Eq. 4.2 is renewed as:

$$\text{P} = \frac{1}{2}(\text{mass flow rate per second})(V^2 - {V_0}^2) \tag{4.3}$$

Also, Mass flow rate can be found from following formula:

$$\text{Mass flow rate} = \rho . A \cdot \frac{V + V_0}{2} \tag{4.4}$$

where:

ρ: Air density ($^{kg}/_{m^3}$)

A: Swept area (m^2)

Area which is captured by turbine blades is called swept are and it depends on the length of blade. In the fig. 5, it is illustrated.

Figure 4.1: Swept area configuration of turbine blades

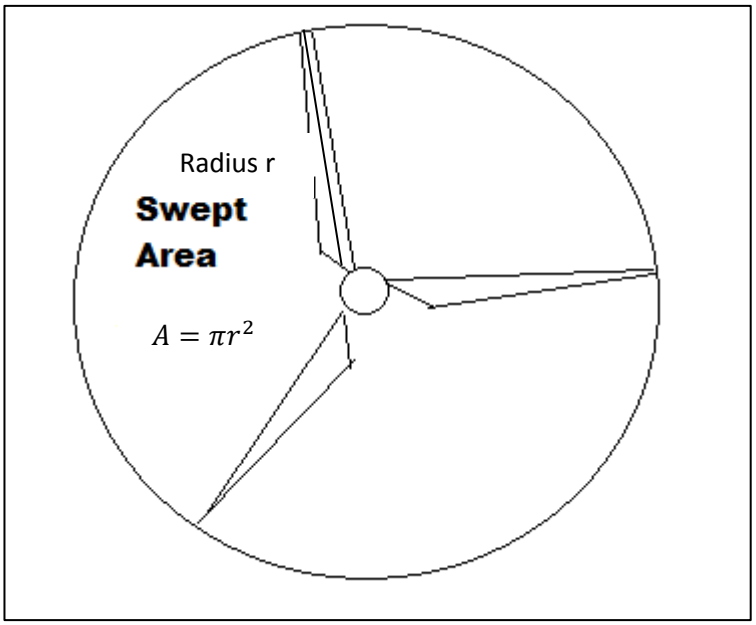

References: Made by O. B. Bekdikhan 2014

When Eq. 4.4 is substituted to Eq. 4.3, following formula is extracted:

$$P = \frac{1}{2}\rho A V^3 C_p \tag{4.5}$$

where:

$C_p = \frac{(1+\frac{V_0}{V})(1-(\frac{V_0}{V})^2)}{2}$

C_p can be defined as power coefficient of the wind turbine. It occurs because of the wind speed difference between entrance and behind of turbine. Therefore, it depends on turbine pitch angle (β) and the tip speed ratio (λ).

C_p can be calculated from lots of different non-linear functions. However, all of them depend on β and λ. Following formula is one of the most popular (Jing 2009).

$$C_p = 0.22\left(\frac{116}{\lambda_i} - 0.4\beta - 5\right)e^{-12.5/\lambda_i} \tag{4.6}$$

In theory, according to Betz law, it cannot be exceed 0.59. It means that none of wind turbine converts more than 59% of kinetic energy to mechanical energy. However, in real applications, the maximum C_p value is between 0.4 and 0.5 (Ofualagba and Ubeku 2008).

4.2 MATHEMATICAL MODEL OF DOUBLY-FED INDUCTION GENERATOR

Nowadays, Doubly-Fed Induction Generator (DFIG) is most popular for wind turbines. The reasons of it and its properties were described in section 1.3. Therefore, DFIG based wind farms are examined in this thesis. DFIGs generally are wound rotor so they have slip rings. Like squirrel cage induction machine, speed of magnetic field and speed of rotor aren't same so they have different positions. Therefore, equations of rotor and stator are not same. These dynamics of DFIG were expressed in many studies (Pierik and others 2004, Jing 2009, Luna and others 2011). Mathematical model of DFIG is expressed in followings.

For stator;

$$v_a = R_s i_a + \frac{d\varphi_a}{dt}$$

$$v_b = R_s i_b + \frac{d\varphi_b}{dt} \tag{4.7}$$

$$v_c = R_s i_c + \frac{d\varphi_c}{dt}$$

For rotor;

$$v_a = R_r i_a + \frac{d\varphi_a}{dt}$$

$$v_b = R_r i_b + \frac{d\varphi_b}{dt} \tag{4.8}$$

$$v_c = R_r i_c + \frac{d\varphi_c}{dt}$$

Also, eq. 4.7 and 4.8 can be written in matrix form. Resistance and inductance matrices for both stator and rotor are below:

$$R_s^{abc} = \begin{bmatrix} R_s & 0 & 0 \\ 0 & R_s & 0 \\ 0 & 0 & R_s \end{bmatrix} \tag{4.9}$$

$$R_r^{abc} = \begin{bmatrix} R_r & 0 & 0 \\ 0 & R_r & 0 \\ 0 & 0 & R_r \end{bmatrix} \tag{4.10}$$

$$L_s^{abc} = \begin{bmatrix} L_s & L_{ms} & L_{ms} \\ L_{ms} & L_s & L_{ms} \\ L_{ms} & L_{ms} & L_s \end{bmatrix} \tag{4.11}$$

$$L_r^{abc} = \begin{bmatrix} L_r & L_{mr} & L_{mr} \\ L_{mr} & L_r & L_{mr} \\ L_{mr} & L_{mr} & L_r \end{bmatrix} \tag{4.12}$$

where:

L_s : self-inductance of stator windings

L_r : self-inductance of rotor windings

L_{ms} : magnetizing inductance of stator windings

L_{mr} : magnetizing inductance of rotor windings

These inductances can be gathered as:

$$[L] = \begin{bmatrix} L_s & L_{ms} & L_{ms} & L_{sr} & L_{sr} & L_{sr} \\ L_{ms} & L_s & L_{ms} & L_{sr} & L_{sr} & L_{sr} \\ L_{ms} & L_{ms} & L_s & L_{sr} & L_{sr} & L_{sr} \\ L_{rs} & L_{rs} & L_{rs} & L_r & L_{mr} & L_{mr} \\ L_{rs} & L_{rs} & L_{rs} & L_{mr} & L_r & L_{mr} \\ L_{rs} & L_{rs} & L_{rs} & L_{mr} & L_{mr} & L_r \end{bmatrix} \tag{4.13}$$

Also, eq. 4.13 can be separated in four sub-matrices.

$$[L] = \begin{bmatrix} L_s & L_{sr} \\ L_{rs} & L_r \end{bmatrix} \tag{4.14}$$

L_{sr} can be defined as:

$$L_{sr} = M_{sr} \begin{bmatrix} \cos(\theta_r) & \cos(\theta_r + \frac{2\pi}{3}) & \cos(\theta_r - \frac{2\pi}{3}) \\ \cos(\theta_r - \frac{2\pi}{3}) & \cos(\theta_r) & \cos(\theta_r + \frac{2\pi}{3}) \\ \cos(\theta_r + \frac{2\pi}{3}) & \cos(\theta_r - \frac{2\pi}{3}) & \cos(\theta_r) \end{bmatrix} \tag{4.15}$$

Inductance between rotor and stator (L_{rs}) is equal to transpose of inductance between stator and rotor (L_{sr}).

$$L_{rs} = (L_{sr})^T = M_{sr} \begin{bmatrix} \cos(\theta_r) & \cos(\theta_r - \frac{2\pi}{3}) & \cos(\theta_r + \frac{2\pi}{3}) \\ \cos(\theta_r + \frac{2\pi}{3}) & \cos(\theta_r) & \cos(\theta_r - \frac{2\pi}{3}) \\ \cos(\theta_r - \frac{2\pi}{3}) & \cos(\theta_r + \frac{2\pi}{3}) & \cos(\theta_r) \end{bmatrix} \tag{4.16}$$

Now, flux linkages can be expressed as:

$$\begin{bmatrix}\varphi_{as}\\ \varphi_{bs}\\ \varphi_{cs}\\ \varphi_{ar}\\ \varphi_{br}\\ \varphi_{cr}\end{bmatrix} = \begin{bmatrix} L_s & 0 & 0 & & L_{sr} & \\ 0 & L_s & 0 & & & \\ 0 & 0 & L_s & & & \\ & & & L_r & 0 & 0 \\ & {L_{sr}}^T & & 0 & L_r & 0 \\ & & & 0 & L_0 & L_r \end{bmatrix} \begin{bmatrix} i_{as}\\ i_{bs}\\ i_{cs}\\ i_{ar}\\ i_{br}\\ i_{cr}\end{bmatrix} \tag{4.17}$$

It can be clearly seen that flux linkages depend on L_{sr}. Also, from 4.15, L_{sr} depends on rotor position θ. Rotor position θ changes with time. Therefore, L_{sr} and accordingly flux linkages depend on time too. In order to make nonlinear time independent equations, these equations should be referred to a reference frame. Thus, simulations can be achieved more quickly. Therefore, Park's transformation or *dq0* transformation is used. The purpose of Park's transformation can be explained as transforming stator variables to a dq reference frame and this dq frame is fixed to the rotor. Park's transformation matrix is below (Kundur 1994, Tacer 1990):

$$[P] = \frac{2}{3}\begin{bmatrix} cos\theta & \cos\left(\theta - \frac{2\pi}{3}\right) & \cos\left(\theta + \frac{2\pi}{3}\right) \\ -sin\theta & -\sin\left(\theta - \frac{2\pi}{3}\right) & -\sin\left(\theta + \frac{2\pi}{3}\right) \\ \frac{1}{2} & \frac{1}{2} & \frac{1}{2} \end{bmatrix} \tag{4.18}$$

where;

θ: angular displacement of Park's reference frame

Park's transformation is applied as:

$$\begin{bmatrix} f_d \\ f_q \\ f_0 \end{bmatrix} = [P] \begin{bmatrix} f_a \\ f_b \\ f_c \end{bmatrix} \tag{4.19}$$

Park's transformation is used for making time and position independent equations. Therefore, in eq. 4.18, f can be i, v or φ. Voltage equations are defined at eq. 4.7 and 4.8. Transformation is applied as:

$$[v_{dq0}] = [P][v_{abc}] \tag{4.20}$$

For stator;

$$\left[v_{dq0s}\right] = [P]Ri_{abcs} + [P]\frac{d}{dt}[\varphi_{abcs}] \tag{4.21}$$

In eq 4.20, $i_{abcs} = [P]^{-1}i_{dq0}$ and , $\varphi_{abcs} = [P]^{-1}\varphi_{dq0}$. When they are applied, eq 4.20 is rewritten as:

$$\left[v_{dq0s}\right] = [P]R[P]^{-1}i_{dq0s} + [P]\frac{d}{dt}[P]^{-1}\left[\varphi_{dq0s}\right] \tag{4.22}$$

However, multiplication of a matrix and its inverse is equal to unit matrix so eq. 4.21 can be rewritten as:

$$\left[v_{dq0s}\right] = Ri_{dq0s} + [P]\frac{d}{dt}[P]^{-1}\left[\varphi_{dq0s}\right] \tag{4.23}$$

According to product rule of derivative, eq 4.22 is renewed as:

$$\left[v_{dq0s}\right] = Ri_{dq0s} + \frac{d}{dt}\left[\varphi_{dq0s}\right] + [P]\frac{d}{dt}[P]^{-1}\left[\varphi_{dq0s}\right] \tag{4.24}$$

where,

$$[P]\frac{d}{dt}[P]^{-1} = \begin{bmatrix} 0 & -\frac{d\theta}{dt} & 0 \\ \frac{d\theta}{dt} & 0 & 0 \\ 0 & 0 & 0 \end{bmatrix}$$

In the above matrix, $\frac{d\theta}{dt}$ is changing of θ. With θ, position of the rotor is specified. Therefore, changing in θ gives angular velocity of rotor. It means $\omega = \frac{d\theta}{dt}$. According to this, eq 4.23 is organized in matrix form as:

$$\begin{bmatrix} v_{ds} \\ v_{qs} \\ v_{0s} \end{bmatrix} = \begin{bmatrix} R & 0 & 0 \\ 0 & R & 0 \\ 0 & 0 & R \end{bmatrix}\begin{bmatrix} i_{ds} \\ i_{qs} \\ i_{0s} \end{bmatrix} + \begin{bmatrix} 0 & -\omega & 0 \\ \omega & 0 & 0 \\ 0 & 0 & 0 \end{bmatrix}\begin{bmatrix} \varphi_{ds} \\ \varphi_{qs} \\ \varphi_{0s} \end{bmatrix} + \frac{d}{dt}\begin{bmatrix} \varphi_{ds} \\ \varphi_{qs} \\ \varphi_{0s} \end{bmatrix} \tag{4.25}$$

When they are written in equation form, all voltages are expressed as:

$$v_{ds} = Ri_{ds} - \omega\varphi_{qs} + \frac{d}{dt}\varphi_{ds} \tag{4.26}$$

$$v_{qs} = Ri_{qs} + \omega\varphi_{ds} + \frac{d}{dt}\varphi_{qs} \tag{4.27}$$

$$v_{0s} = Ri_{0s} + \frac{d}{dt}\varphi_{0s} \tag{4.28}$$

From eq.4.20 to eq4.23 is same for the rotor. However, for rotor, $\omega - \omega_r = \frac{d\theta}{dt}$. In here;

ω is again rotational speed of reference frame

ω_r is rotational speed of the rotor

According to this, eq 4.24 can be written for rotor as:

$$\begin{bmatrix} v_{dr} \\ v_{qr} \\ v_{0r} \end{bmatrix} = \begin{bmatrix} R & 0 & 0 \\ 0 & R & 0 \\ 0 & 0 & R \end{bmatrix} \begin{bmatrix} i_{dr} \\ i_{qr} \\ i_{0r} \end{bmatrix} + \begin{bmatrix} 0 & -\omega - \omega_r & 0 \\ \omega - \omega_r & 0 & 0 \\ 0 & 0 & 0 \end{bmatrix} \begin{bmatrix} \varphi_{dr} \\ \varphi_{qr} \\ \varphi_{0r} \end{bmatrix} + \frac{d}{dt} \begin{bmatrix} \varphi_{dr} \\ \varphi_{qr} \\ \varphi_{0r} \end{bmatrix} \tag{4.29}$$

Also, it can be written as equation form:

$$v_{dr} = 0 = Ri_{dr} - (\omega - \omega_r)\varphi_{qr} + \frac{d}{dt}\varphi_{dr} \tag{4.30}$$

$$v_{qr} = 0 = Ri_{qr} + (\omega - \omega_r)\varphi_{dr} + \frac{d}{dt}\varphi_{qr} \tag{4.31}$$

$$v_{0r} = 0 = Ri_{0r} + \frac{d}{dt}\varphi_{0r} \tag{4.32}$$

Expression on the above is for rotor of DFIG. After all transformations, torque equation can be defined. Electrical torque is:

$$T_e = \frac{3}{2}\left(\frac{P}{2}\right)\left(\varphi_{qr}i_{dr} - \varphi_{dr}i_{qr}\right) \tag{4.33}$$

In here, p is the number of poles.

$$J\frac{d\omega_r}{dt} = (T_e - T_m) \tag{4.34}$$

where;

J: moment of inertia

T_m: mechanical torque (torque which is connected to shaft)

From these torque equations, following active and reactive power equations can be obtained.

$$P_s = v_{ds}i_{ds} + v_{qs}i_{qs} \tag{4.40}$$

$$Q_s = v_{ds}i_{qs} - v_{qs}i_{ds} \tag{4.41}$$

5. VOLTAGE STABILITY

With technological developments and increasing population, energy demand of world is getting increase. In order to meet this demand, lots of new power generators are put into use. While production capacity is increasing, transmission and distribution systems are developed too. This growth causes lots of problem. Voltage stability problem is the one of the important. Huge electricity system networks collapse in recent years because of the stability problems. Therefore, stability studies take attention nowadays.

In the literature, voltage stability can be defined lots of different ways. Basically, it can be explained as keeping voltages of all buses in acceptable limits. Under normal conditions and also after a fault, if voltages at all buses of a power system are not exceeding the acceptable limits, system is stable. Also, voltage stability of a system can be controlled with reactive power injection. When reactive power injection is increased, voltages at the all buses should be increase in order to be called stable. Even one of them decrease, system has voltage instability. There are many reasons which cause voltage instability such as increase in load, voltage drops. However, the main reason is reactive power demand. If power system cannot meet the reactive power demand, voltage instability occur. Active and reactive power flow at the transmission networks cause voltage drops and accordingly voltage instability (Kundur 1994).

Lots of different problems can cause voltage instability. These problems can affect system's stability in different time period. Therefore, while analyzing a power system's stability, these problems should be classified. Voltage stability can be divided into four groups: *small disturbance voltage stability*, *large disturbance voltage stability*, *transient voltage stability* and *long term voltage stability*.

5.1 SMALL DISTURBANCE VOLTAGE STABILITY

In order to call a system voltage stable, voltages cannot exceed limits no only normal conditions but also after fault conditions. Accordingly, small disturbance voltage stability can be defined that system stay stable after a small disturbance occur. Increase in system's load is main example of small disturbances. Therefore, while this type stability is analyzing, load characteristics are examined (Kundur 1994).

5.2 LARGE DISTURBANCE VOLTAGE STABILITY

System faults, loss of generation and circuit contingencies are most common large disturbance. If a power system can control all bus voltages after this type disturbance, the system has ability of large disturbance voltage stability. While this type stability analysis is performing, system-load characteristics and control-protection coordination should be examined (Kundur 1994).

Both small and large disturbances occur at different time scales. Therefore, according to their time, voltage stability can be separated as transient and long term stability. In the following figure, some disturbance and their clearing times are specified in these two groups.

Figure 5.1: Time response for classification of voltage stability

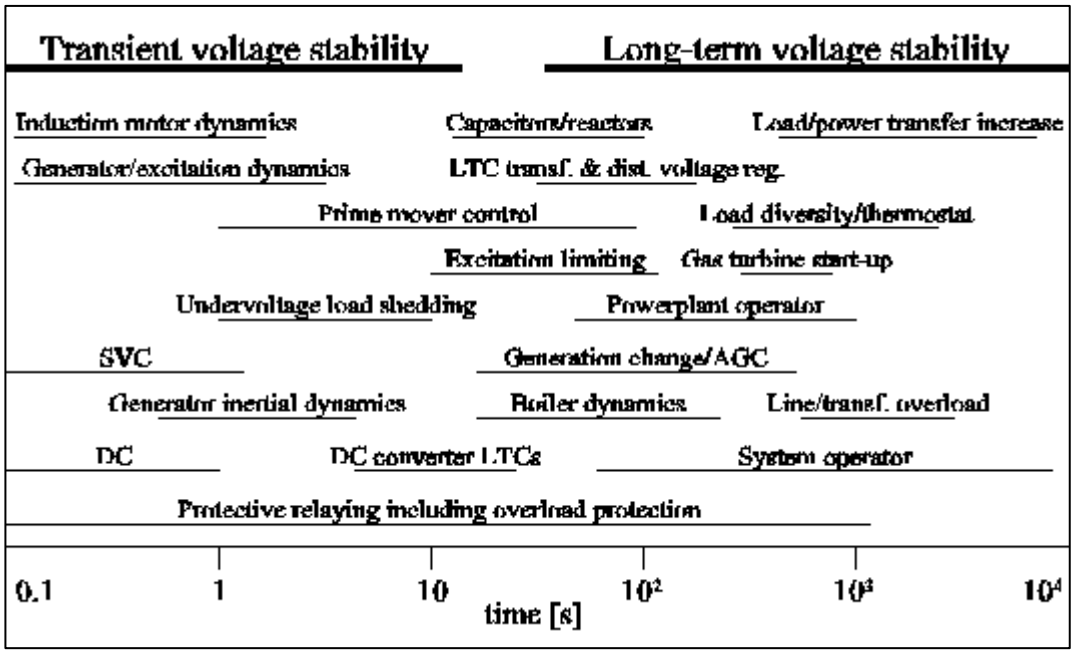

Reference: Kundur, 1994

5.3 TRANSIENT VOLTAGE STABILITY

Time scale of transient voltage stability is between zero and ten seconds. Transient voltage stability is mainly depended on induction motors. Because when a fault occurs, electrical torque cannot meet the required mechanical torque. However, in recent years,

effects of high voltage direct current (HVDC) links are founded. HVDC links can cause transient voltage stability problems when used in weak systems. Also, inverters and shunt capacitors lead to voltage instability (Padiyar 2004).

5.4 LONG TERM VOLTAGE STABILITY

Time scale of long term voltage stability is between ten seconds and two-three minutes. Loss of large generators and contingency of a transmission line are most common scenarios of this type stability. These situations cause reactive power losses and voltage sags. Therefore, on load tap changing transformers and distribution voltage regulators are used to fix these sags (Kundur 1994).

6. STATIC ANALYSIS OF VOLTAGE STABILITY

In recent years, voltage collapse which occurs because of voltage instability cause cut-out of huge electricity systems. When a huge system collapses, it takes long time to fix again. Therefore, voltage stability analysis methods take attention in last decade. Voltage stability is both static and dynamic phenomena. Most common static analysis methods are P-V curve method, V-Q curve method, based on singularity of power flow Jacobian matrix and continuation power flow method. This thesis focuses on continuation power flow method. However, in order to understand it, firstly bifurcation theory should be explained.

6.1 BIFURCATION THEORY

In a dynamic system, when system parameters are changed, structure of the phase portrait changes. This is the basic explanation of bifurcation term. In order to examine local bifurcations, vector differential equations which are near the bifurcation point are analyzed. While doing this analysis, a loading parameter λ should be specified. In a power system, changing in λ means system's load changes. Accordingly, active and reactive power changes too.

Bifurcation can be defined by eq. 6.1.

$$\dot{x} = \lambda - x^2 = f(x, \lambda) \tag{6.1}$$

In this equation, x is the state variable. With changings inλ, $f(x, \lambda)$ changes. A diagram shows this relationship is illustrated in figure 6.1. If λ<0, equilibrium is not provided. If λ>0, two equilibrium points are obtained. One of them is for stable point and the other is the unstable point. When λ=0, equilibrium point is get and at this point, stability situation of the system change. At the equilibrium (0, 0) or in other words steady-state voltage stability limit, linearization of $f(x, \lambda)$ is singular. Therefore, it is unsolvable. In order to avoid this singularity, continuation power flow method is used (Canizares 1991).

Figure 6.1: Bifurcation diagram of f(x,λ)

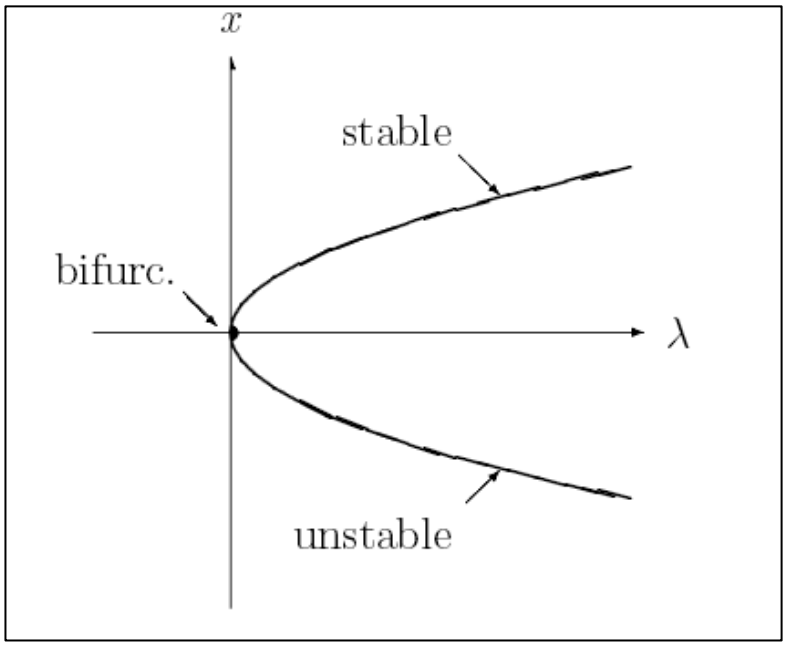

Reference: Canizares 1991

6.2 CONTINUATION POWER FLOW

Continuation power flow is a method that examines steady-state behavior of a power system under load and generation changings. This method can be used in lots of different situation but especially, it is used to analyze voltage changings and maximum capability under different load and generation conditions (Chiang and others 1995).

Principles of this method based on bifurcation theory which is explained in last section. As mentioned before, there is a problem while doing steady-state voltage stability analysis. In this analysis, conventional Newton-Raphson power flow techniques are modified. However, Jacobian matrix becomes singular and it cannot be solved at the voltage stability limit. This limit also called as critical point. In summary, near the critical point, power flow solutions are unsolvable. Therefore, power flow equations should be reformulated by using continuation power flow method.

In the continuation power flow method, a load parameter λ is inserted to the power flow equations. Then, in order to find solution path of reformulated power flow equations, a predictor-corrector process are applied. In figure 6.2, predictor-corrector process is

illustrated. Firstly, initial base is found from conventional power flow. This initial solution is used to start. Then, a tangent predictor is applied at the different load parameter and solution is predicted. After the prediction, correction step is applied. This process goes on until the critical point. In summary, continuation power flow method can be divided into four steps (Ajjarapu and Christy 1992):

i. Parameterization
ii. Predictor
iii. Corrector
iv. Step-size control

Figure 6.2: Predictor-Corrector process in continuation power flow

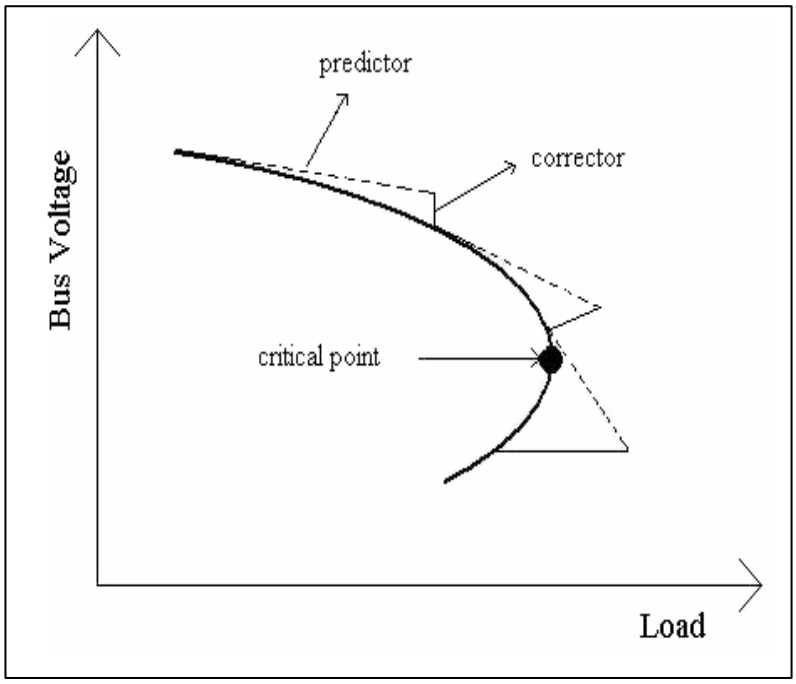

Reference: Ajjarapu and Christy 1992

6.2.1 Reformulation of Power Flow Equations

As mentioned before, continuation power flow technique can be separated into four steps. First step is parameterization. A load parameter has to be inserted into power flow equations. Thus, generation and load at a bus are defined as a function of load parameter λ. Conventional power flow equations for bus i are below.

$$P_{Gi} - P_{Li} - P_{Ti} = 0 \qquad (6.2)$$

$$Q_{Gi} - Q_{Li} - Q_{Ti} = 0 \tag{6.3}$$

For parameterization, λ is inserted into equations 6.2 and 6.3 for each bus I of an n bus system.

$$P_{Gi}(\lambda) - P_{Li}(\lambda) - P_{Ti} = 0 \tag{6.4}$$

$$Q_{Gi} - Q_{Li}(\lambda) - Q_{Ti} = 0 \tag{6.5}$$

where;

$$P_{Ti} = \sum_{j=1}^{n} V_i\, V_j\, y_{ij} \cos(\delta_i - \delta_j - \gamma_{ij})$$

$$Q_{Ti} = \sum_{j=1}^{n} V_i\, V_j\, y_{ij} \sin(\delta_i - \delta_j - \gamma_{ij})$$

In the equations, G, L and T respectively represent bus generation, load and injection. Also, y_{ij} represents (i, j)th element of system admittance matrix $Y_{BUS.}$ Effect of load change can be shown clearly by revising P_{Li} and Q_{Li}.

$$P_{Li} = P_{Li0} + \lambda(k_{Li} S_{\Delta base} cos\varphi_i) \tag{6.6}$$

$$Q_{Li} = Q_{Li0} + \lambda(k_{Li} S_{\Delta base} sin\varphi_i) \tag{6.7}$$

where,

P_{Li0}, Q_{Li0}: initial values of active and reactive loads

k_{Li} : multiplier which specify load change rate at bus i while λ is changing

φ_i : at bus i, load change's power factor angle

$S_{\Delta base}$: apparent power for calculating proper λ value

Also, in equation 4.6, $S_{\Delta base} cos\varphi_i = P_{Li0}$ and in equation 4.7, $S_{\Delta base} sin\varphi_i = Q_{Li0}$. According to these, they can be rewritten. However, these equations are organized for loads. For active power generation, following equation can be used:

$$P_{Gi} = P_{Gi0}(1 + \lambda k_{Gi}) \tag{6.8}$$

where,

P_{Gi0}: initial value of active power generation at bus i

k_{Gi}: constant which determines rate of generation change while λ is varying

If equations 6.6, 6.7 and 6.8 are put into equations 6.4 and 6.5, new power flow equations are obtained.

$$0 = P_{Gi0}(1 + \lambda k_{Gi}) - P_{Li0} - \lambda(k_{Li} S_{\Delta base} cos\varphi_i) - P_{Ti} \tag{6.9}$$

$$0 = Q_{Gi0} - Q_{Li0} - \lambda(k_{Li} S_{\Delta base} sin\varphi_i) - Q_{Ti} \tag{6.10}$$

Also, these new equations can be expressed in vector form and thus continuation algorithm can apply. Equations set can be represented as $\underline{F}$, and can be written as

$$\underline{F}(\underline{\delta}, \underline{V}, \lambda) = 0, \qquad 0 \leq \lambda \leq \lambda_{critical}$$

where:

$\underline{\delta}$: bus voltage angles' vector

$\underline{V}$: bus voltage magnitudes' vector

Basically, a known solution (initial values) which is found from conventional power flow is used for continuation algorithm in first step and then secondly, predictor-corrector process starts (Ajjarapu and Christy 1992).

6.2.2 Prediction Step

After the initial solution usage and parameterization, prediction step starts. In this step, a proper point for the next solution is found. This is achieved by taking tangent vector to the solution path. Therefore, firstly tangent vector should be calculated. In order to calculate it, derivative of power flow equations are taken.

$$d\left[\underline{F}\left(\underline{\delta},\underline{V},\lambda\right)\right] = \underline{F_{\delta}}d\underline{\delta} + \underline{F_{V}}d\underline{V} + \underline{F_{\lambda}}d\lambda = \underline{0}$$

Also, it can be written in vector form;

$$[\underline{F_{\delta}} \quad \underline{F_{V}} \quad \underline{F_{\lambda}}]\begin{bmatrix} d\underline{\delta} \\ d\underline{V} \\ d\lambda \end{bmatrix} = 0 \tag{6.11}$$

In order to avoid singularity of Jacobian matrix, a parameter λ is inserted in the power flow equations as above. However, a new problem occurs in this situation. A parameter (an additional unknown) λ is inserted but the number of equations is still same so the problem cannot be solved. In order to solve this, a new equation is needed. If one of the tangent vector components is taken as +1 or -1, problem can be fixed. It can be shown as following:

$$\begin{bmatrix} \underline{F_{\delta}} & \underline{F_{V}} & \underline{F_{\lambda}} \\ & \underline{e_k} & \end{bmatrix}\begin{bmatrix} \\ t \\ \\ \end{bmatrix} = \begin{bmatrix} \underline{0} \\ \mp 1 \end{bmatrix} \tag{6.12}$$

where;

t : tangent vector, $\begin{bmatrix} d\underline{\delta} \\ d\underline{V} \\ d\lambda \end{bmatrix}$

$\underline{e_k}$: a row vector which kth element is one and the others are zero

After the tangent vector calculation, prediction is achieved as following:

$$\begin{bmatrix} \underline{\delta} \\ \underline{V} \\ \lambda \end{bmatrix}^{p} = \begin{bmatrix} \underline{\delta} \\ \underline{V} \\ \lambda \end{bmatrix} + \sigma \begin{bmatrix} d\underline{\delta} \\ d\underline{V} \\ d\lambda \end{bmatrix} \tag{6.13}$$

In the above, p is the predicted values and σ is the step size which specified for the next point. There are lots of different methods for specifying σ but generally a constant magnitude for it is used (Ajjarapu and Christy 1992).

6.2.3 Correction Step

After the prediction step, correction step starts. The purpose of this step is correcting the predicting solution. This correction generally is achieved by local parameterization. Local parameterization is applied on power flow equations which get additional equation in predictor. Thus;

$$\begin{bmatrix} \underline{F}(\underline{x}) \\ x_k - \eta \end{bmatrix} = \begin{bmatrix} \underline{0} \end{bmatrix} \tag{6.14}$$

where;

x_k : a state variable as continuation parameter

η : predicted value for this state variable

Firstly, proper values for k and η are selected, then solution is obtained by slightly modified Newton-Raphson power flow method.

6.2.4 Step Size Control

In general, continuation parameter is selected according to largest vector component. When process starts from base solution, λ can be a good choice. For the other parameters, following formula is used.

$$x_k : |t_k| = max\{|t_1|, |t_2|, \dots, |t_m|\} \tag{6.15}$$

On the above, t is the tangent vector and the dimension of it is $m = 2n_1 + n_2 + 1$. If following tangent vector is increasing, t_k is +1. If it is decreasing, t_k becomes -1.

All CPF process is summarized in the figure 6.3.

Figure 6.3: CPF process flow chart

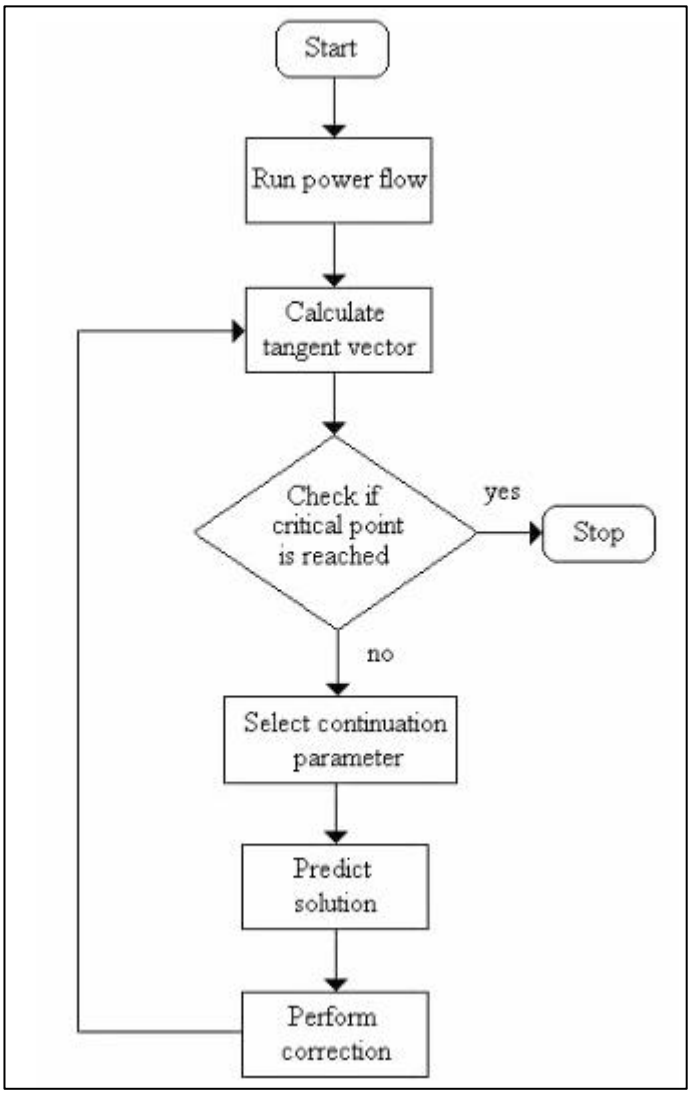

Reference: Keskin 2007

7. DYNAMIC ANALYSIS OF VOLTAGE STABILITY

In the literature, voltage stability assessments generally were achieved statically. However, voltage stability is both static and dynamic phenomena. Principles of this dynamic analysis depend on time domain solutions of power systems. Thus, system components' effects which occur in time can be observed, also, faults can be cleared before voltage collapse. There are lots of components which have dynamic effects such as controllers, on-load-tap-changers etc.

Time domain solutions are practiced by solving differential algebraic equations. However, power systems consist of many dynamic components and all of them have differential equations so huge number of equations should be solved for this analysis. Therefore, computer programs usage is significant. Despite these difficulties, dynamic analysis must be made for more reliable power systems. Thanks to this analysis, voltage collapse can be avoided by arranging controllers and etc. (Hasani and Parniani 2005).

7.1 TIME DOMAIN SIMULATIONS

Time domain simulations are used for dynamic/transient stability analysis. In time domain simulations, several differential algebraic equations should be solved. Therefore, numerical integration methods are used. Most common integration methods are Euler, Runge-Kutta and trapezoidal method.

7.1.1 Euler Method

Euler method is applied like in figure 7.1. As it can be seen, method is approximating graph of $y(x)$ with tangent line in step by step. Euler Method is applied to first order differential equations;

$$\frac{dx}{dt} = f(x,t) \tag{7.1}$$

When $x = x_0$ and $t = t_0$, true solution is estimated by tangent's slope

$$\left.\frac{dx}{dt}\right|_{x=x_0} = f(x_0, t_0)$$

So,

$$\Delta x = \left.\frac{dx}{dt}\right|_{x=x_0} . \Delta t$$

When a step is applied which means $t = t_1 = t_0 + \Delta t$, x is equal to

$$x_1 = x_0 + \Delta x = x_0 + \left.\frac{dx}{dt}\right|_{x=x_0} . \Delta t \tag{7.2}$$

The process continues as same way. If step is increased again, then x is equal to

$$x_2 = x_1 + \left.\frac{dx}{dt}\right|_{x=x_1} . \Delta t \tag{7.3}$$

With this method, corresponding x values can be obtained at different values of t. therefore, in power system, with time changing, system's reaction can be understood (Kundur 1994).

Figure 7.1: Euler Method's illustration

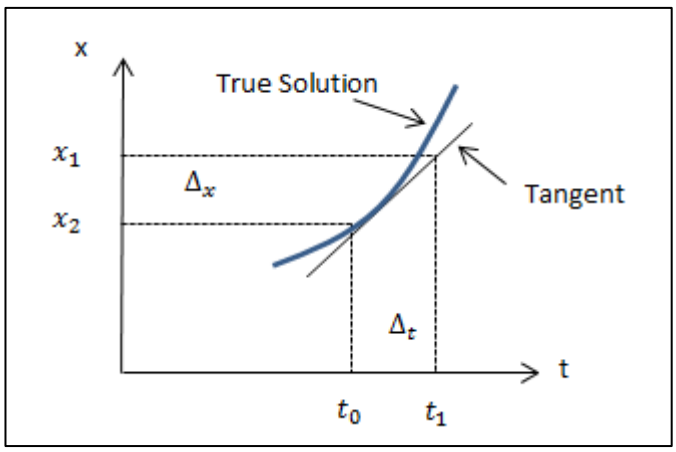

Reference: Made by O. B. Bekdikhan 2014

7.1.2 Runge-Kutta Method

Runge-Kutta (R-K) is one of the favorite methods for solving differential equations. Unlike the Euler method, Runge-Kutta method has single step. However, this step has

more than one stage. This method based on Taylor series solution. Runge-Kutta method can be divided into two categories; second order R-K and fourth order R-K (Kundur 1994).

Second order R-K;

Again, first order differential equation in eq. 7.1 is used. When R-K method is applied at $t = t_0 + \Delta t$, x can be defined as

$$x_1 = x_0 + \Delta x = x_0 + \frac{k_1 + k_2}{2} \tag{7.4}$$

where;

$k_1 = f(x_0, t_0)\Delta t$

$k_2 = f(x_0 + k_1, t_0 + \Delta t)\Delta t$

Fourth order R-K;

Fourth-order model can be defined with the following formula. Formula in the below is written for x values which are at the $(n+1)^{st}$ step.

$$x_{n+1} = x_n + \frac{1}{6}(k_1 + 2k_2 + 2k_3 + k_4) \tag{7.5}$$

where;

$k_1 = f(x_n, t_n)\Delta t$

$k_2 = f(x_n + \frac{k_1}{2}, t_n + \frac{\Delta t}{2})\Delta t$

$k_2 = f(x_n + \frac{k_2}{2}, t_n + \frac{\Delta t}{2})\Delta t$

$k_4 = f(x_n + k_{3,} t_n + \Delta t)\Delta t$

k values represents the slopes at each time step.

7.1.3 Trapezoidal Rule Method

Area under the integral of a function can be estimated with trapezoidal rule. It can be seen from the figure 7.2. It is a quite simple second order method. Trapezoidal rule can be mathematically explained as (Kundur 1994)

$$x_{n+1} = x_n + \frac{\Delta t}{2}[f(x_n, t_n) + f(x_{n+1}, t_{n+1})] \tag{7.6}$$

In the equation 5.6, values of x is written for $t = t_{n+1}$.

Figure 7.2: Trapezoidal Rule

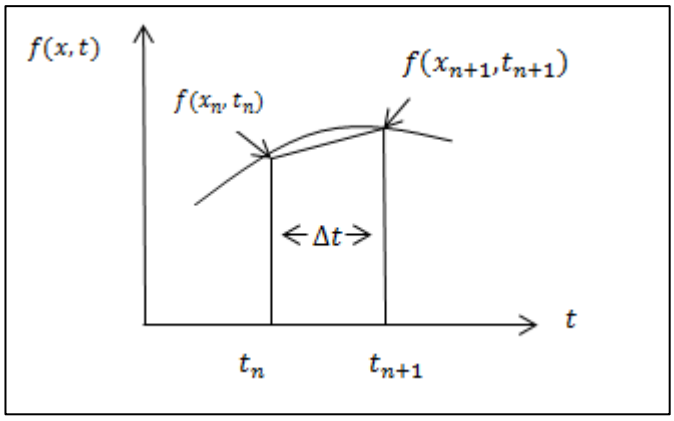

Reference: Made by O. B. Bekdikhan 2014

8. REACTIVE POWER COMPENSATION FOR VOLTAGE STABILITY

Voltage instability is most important power quality problem for power systems. If stability cannot provided quickly, electricity system can collapse and it takes long time for operating again. The main reason which causes voltage instability is reactive power. If a power system cannot meet reactive power requirement, voltage instability occurs. In order to avoid this, reactive power compensation techniques have to be used.

Once, shunt capacitors are widely used for reactive power compensation. However, with technological developments, new techniques are developed. Nowadays, Flexible Alternating Current Transmission Systems (FACTS) are mostly preferred. When they are compared with shunt capacitors, it is seen that they are more effective for reactive power compensation and also voltage stability. There are lots of different FACTS devices but nowadays, SVC, STATCOM, TCSC and UPFC are most popular ones.

8.1 SHUNT CAPACITORS

Shunt capacitors are oldest method for supplying reactive power. The purpose of them is increasing voltage level by supplying reactive power. While doing this, they also contribute the power factor correction. Shunt capacitors are very cheap and simple. They can be used in lots of different point in a system. Thus, efficiency is increasing. However, there are also some disadvantages. Their reactive power supply depends on voltage. When voltage is low, reactive power production is low too (Kundur 1994).

With developments in FACTS devices, nowadays, shunt capacitors become disfavor.

8.2 STATIC VAR COMPENSATOR

Static var compensators consist of static generators or absorbers which are connected as shunt. Therefore, sometimes they are called as shunt controllers. According to arrangement, output of SVC can be inductive or capacitive for controlling. They operate like synchronous compensator so they can give or absorb reactive power from grid. Unlike synchronous compensators, SVC's have not any moving part. Therefore, they called as static. Generally, they are used as two different connections. First one is a fixed capacitor with a thyristor controlled reactor (FC-TCR) usage. The other is a thyristor switched capacitor with thyristor controlled reactor (TSC-TCR) usage. Second

type SVC also known as TCSVC. Configurations of SVC's types are included in figure 8.1 (Kamarposhti and others 2008, Canizares 2000).

Figure 8.1: a) configuration of FC-TCR b) configuration of (TSC-TCR)

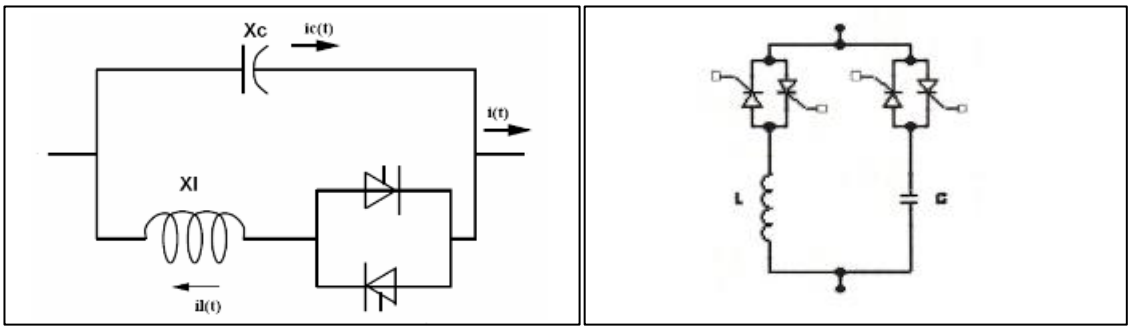

(a) (b)

Reference: Kamarposhti and others 2008, Canizares 2000

SVCs are effective devices for supplying transient stability. Therefore, while doing stability analysis of a power system, model of SVC should be considered. In Fig. 8.2, transient stability model of SVC is illustrated.

Figure 8.2: Model of SVC for transient stability

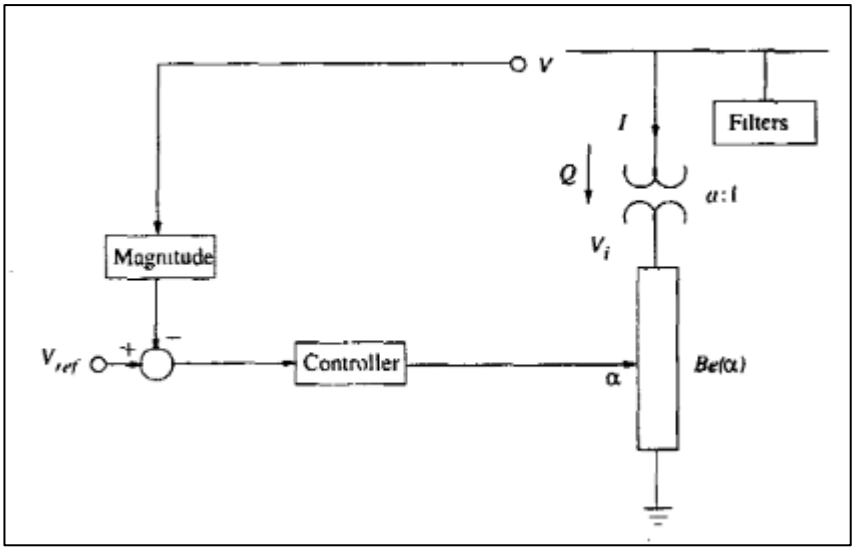

Reference: Canizares 2000

Figure 8.2 mathematically can be shown as

$$\begin{bmatrix} \dot{x_c} \\ \propto \end{bmatrix} = f(x_c, \propto, V, V_{ref}) \tag{8.1}$$

$$\begin{bmatrix} B_e - \dfrac{2 \propto -sin2 \propto -\pi(2 - \dfrac{X_L}{X_C})}{\pi X_L} \\ I - V_i B_e \\ Q - {V_i}^2 B_e \end{bmatrix} \tag{8.2}$$

$$\downarrow$$

$$g(\propto, V, V_i, I, Q, B_e)$$

Also, model of SVC can be modified for steady state conditions. Thus, it can be shown in the power flow.

$$0 = \begin{bmatrix} V - V_{ref} - X_{SL} I \\ g(\propto, V, V_i, I, Q, B_e) \end{bmatrix} \tag{8.3}$$

8.3 STATCOM

STATCOM is a shunt connected FACTS device. It operates as a voltage source inverter. In order to supply active or reactive power, it converts input DC voltage to output AC. When it is applied a bus, it can be give or absorb reactive power for arranging bus voltage. STATCOM consist of a transformer, converter and a DC capacitor. In the structure, DC capacitor is used for supplying DC voltage to the converter. Basic configuration of it is illustrated in figure 8.3.

Figure 8.3: Basic configuration of STATCOM

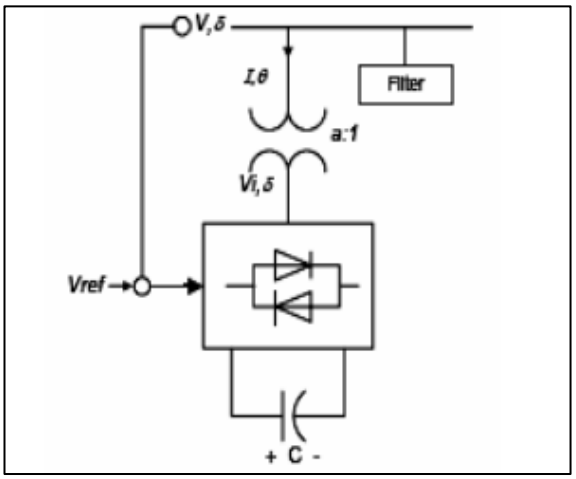

Reference: Kamarposhti and others 2008

As mentioned above, STATCOM can absorb or give reactive power to system for stability. If the magnitude of STATCOM's output voltage is higher than the AC system, current flows from STATCOM to the system via transformer. Thus, STACOM produces reactive power for the grid. In the second case, if the magnitude of STATCOM's output voltage is lower than the AC system, current flows from AC system to the STATCOM. Thus, STATCOM consumes reactive power. This process can be summarized by transient stability model of STATCOM and it is illustrated in figure 8.4 (Kamarposhti and others 2008, Canizares 2000, Ertay and Aydoğmuş 2011).

Figure 8.4: Model of STATCOM for transient stability

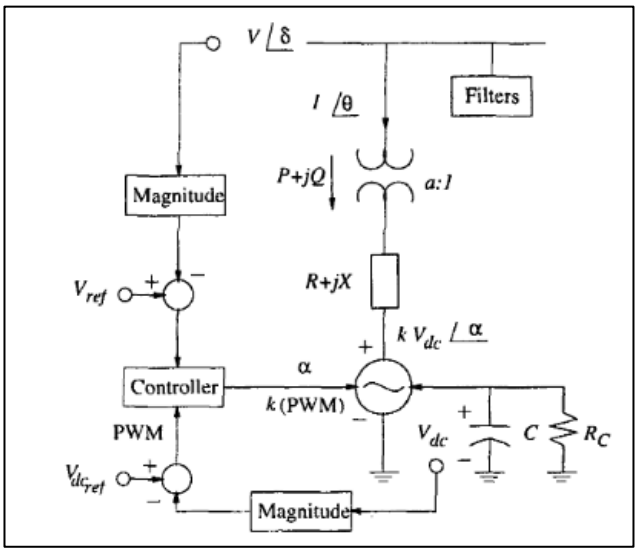

Reference: Canizares 2000

Mathematical model of it;

$$\begin{bmatrix} \dot{x_c} \\ \propto \\ \dot{m} \end{bmatrix} = f\left(x_c, \propto, m, V, V_{dc}, V_{ref}, V_{dc,ref}\right) \tag{8.4}$$

$$\dot{V_{dc}} = \frac{VI}{CV_{dc}}\cos(\delta - \theta) - \frac{1}{R_c C}V_{dc} - \frac{R}{C}\frac{I^2}{V_{dc}} \tag{8.5}$$

$$0 = \begin{bmatrix} P - VI\cos(\delta - \theta) \\ Q - VI\sin(\delta - \theta) \\ P - V^2G + kV_{dc}VGcos(\delta - \theta) + kV_{dc}VBsin(\delta - \theta) \\ Q + V^2B - kV_{dc}VGcos(\delta - \theta) + kV_{dc}VBsin(\delta - \theta) \end{bmatrix} \tag{8.6}$$

$$\downarrow$$

$$g(\alpha, k, V, V_{dc}, \delta, I, \theta, P, Q)$$

In here, $k = \sqrt{\frac{3}{8}}\, m$. m represents pulse width modulation.

Also, this model can be modified for steady state condition. Therefore, it can be used for static voltage stability analysis.

$$0 = \begin{bmatrix} V - V_{ref} \mp X_{SL}I \\ V_{dc} - V_{dc,ref} \\ P - {V_{dc}^2}/{R_c} - RI^2 \\ g(\alpha, k, V, V_{dc}, \delta, I, \theta, P, Q) \end{bmatrix} \tag{8.7}$$

8.4 UPFC

UPFCs consist of two voltage source inverters which use Gate turn off Thyristor. These inverters use a common dc bus. In order to connect these, a shunt transformer and a series transformer are used. UPFC operates as an AC-AC converter. Active power can flow between the terminals of two converters. Each converter can produce or consume reactive power.

UPFC's functions can be categorized as;

i. Control of active reactive power flow
ii. Voltage regulation
iii. Series and shunt compensation
iv. Phase shifting

Unlike the other devices, UPFC is a multifunctional device. With a voltage source injection, it can change line impedance, voltage and phase angle synchronously. However, other devices can achieve this with combined usage (Canizares 2000).

Basic structure of UPFC can be seen from figure 8.5.

Figure 8.5: Scheme of an UPFC

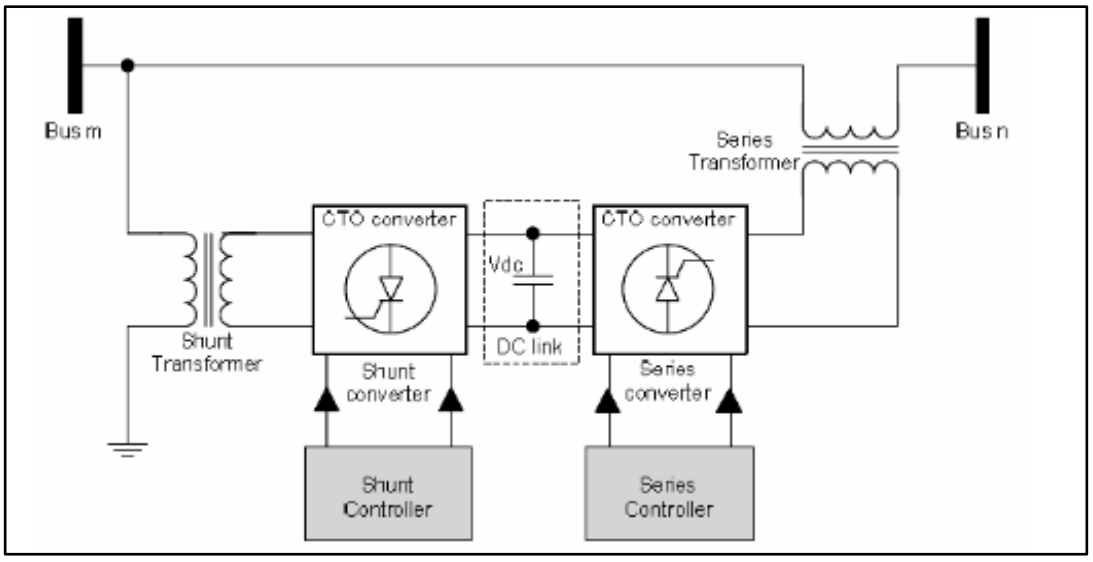

Reference: Ertay and Aydoğmuş 2011

UPFC can be used for voltage stability. Therefore, model of it should be analyzed.

Figure 8.6: Model of an UPFC for transient stability

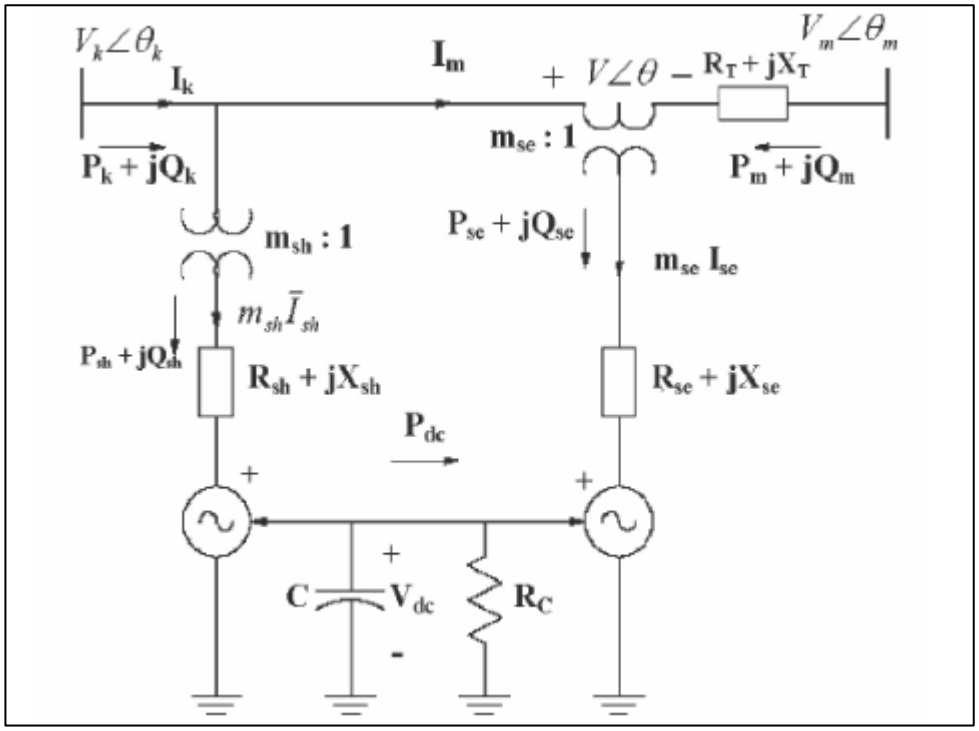

Reference: Canizares 2000

Figure 8.6 can be explained mathematically as;

$$P_k = P_{sh} + \sum\{\overline{V_k I_m^*}\}$$

$$Q_k = Q_{sh} + \sum\{\overline{V_k}\, I_m^*\} \tag{8.8}$$

$$P_m = -\sum \overline{V_m}\, \overline{I_m{}^*}$$

$$Q_k = -\sum \overline{V_m}\, \overline{I_m{}^*}$$

where;

$$P_{sh} = V_k^2 G_{sh} - K_{sh} V_{dc} V_k G_{sh} \cos(\theta_k - \alpha) - K_{sh} V_{dc} V_k B_{sh} \sin(\theta_k - \alpha)$$

$$Q_{sh} = V_k^2 B_{sh} - K_{sh} V_{dc} V_k B_{sh} \cos(\theta_k - \alpha) - K_{sh} V_{dc} V_k G_{sh} \sin(\theta_k - \alpha)$$

9. SIMULATIONS IN PSAT

As mentioned in previous sections, several differential equations have to be solved for analyzing a power system. In order to solve DAEs in short period, simulation programs are developed. Both dynamic and static analyzes can be achieved by them. In this thesis, PSAT program is preferred for simulations.

PSAT also known as Power System Analysis Toolbox is MATLAB/Simulink based program. It was developed by Dr. Federico Milano in 2002. It is completely free and open source software program. PSAT was designed to operate as graphical user interfaces. Thus, it is easy to use.

Generally, similar programs can achieve only static or only dynamic simulations. However, PSAT can analyze a system statically and dynamically at the same time. This is the major advantage of it. Another important advantage is dynamic components model. It has lots of dynamic component models such as wind turbines, FACTS devices, voltage regulators etc. Functions of PSAT can be ordered as;

i. Power Flow
ii. Continuation Power Flow
iii. Optimal Power Flow
iv. Small Signal Stability Analysis
v. Time Domain Simulations
vi. Phasor Measurement Unit (PMU) Placement

Because of these features, PSAT is selected for analyzing power systems in this thesis. However, firstly, accuracy test of PSAT is completed. In this process, IEEE 9 bus test system is used as case study. Data of IEEE 9 bus test system can be found in Appendix D.

9.1 POWER FLOW ANALYSIS OF IEEE 9-BUS TEST SYSTEM IN PSAT

The purpose of this thesis is assessing voltage stability of wind farms in a real grid. Both static and dynamic analyzes are completed in PSAT. However, before making assessment on the real Turkish electricity system, firstly reliability of PSAT should be proved. Therefore, a test system which is known its result should be simulated. IEEE 9-bus test system is selected for this purpose. There are two model of this test system. One of them is simple and the other is more detail. Detail model which also known as WSCC is preferred. This system consists of 9 buses and 3 generators. Base apparent power and base frequency are 100 MVA and 60 Hz respectively. Model of 9 bus test system and parameters can be seen from figure 9.1.

Figure 9.1: IEEE 9 bus test system configuration and data

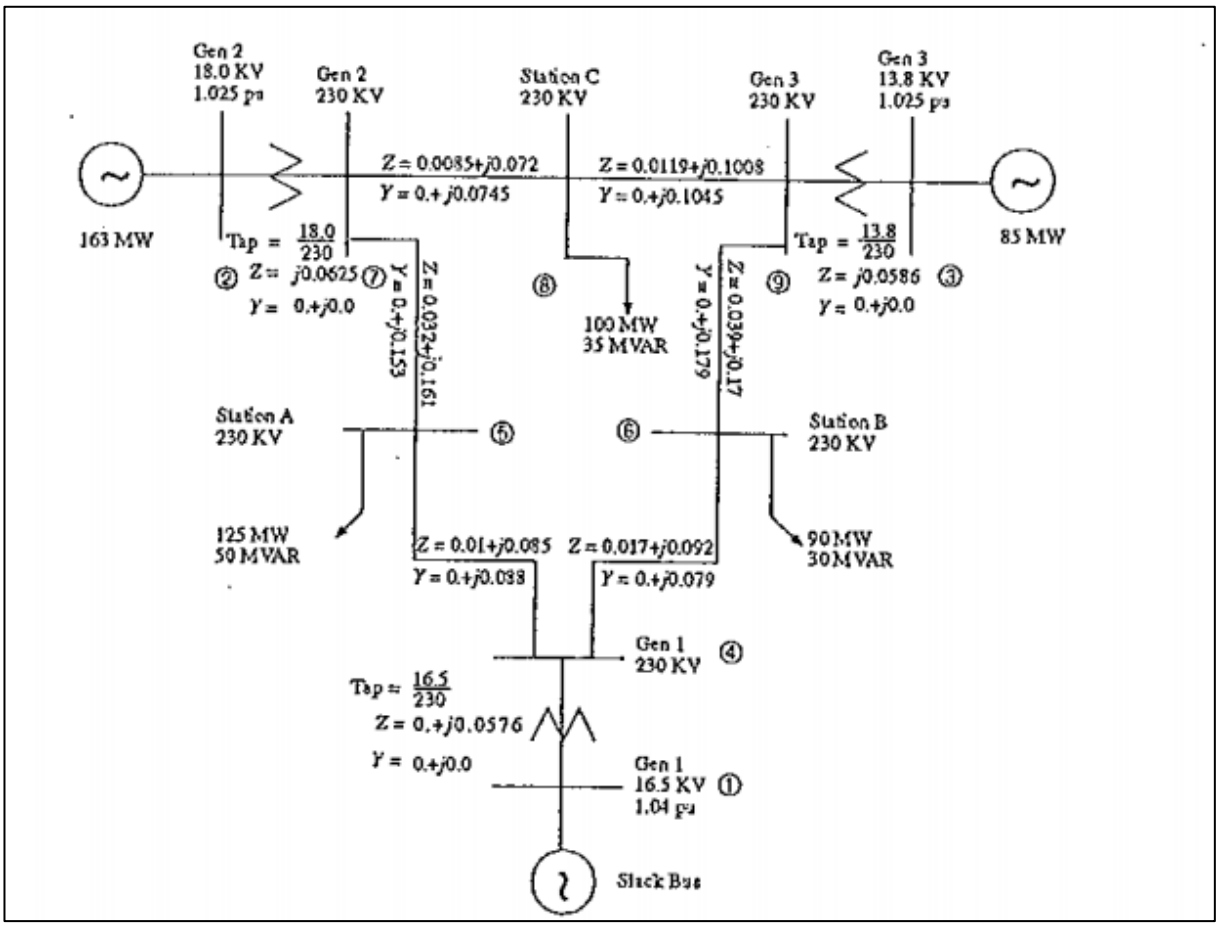

Reference: Sauer and Pai 1998

PSAT model of 9 bus test system is illustrated in figure 9.2. After model is created, power flow is completed by using Newton-Raphson method in PSAT. Power flow results are given in Table 9.1. When it compares with IEEE results, it is found that true solutions are obtained. Thus, reliability of PSAT is proven. IEEE results can be found in (Sauer and Pai 1998).

Figure 9.2: PSAT model of IEEE 9-bus test system

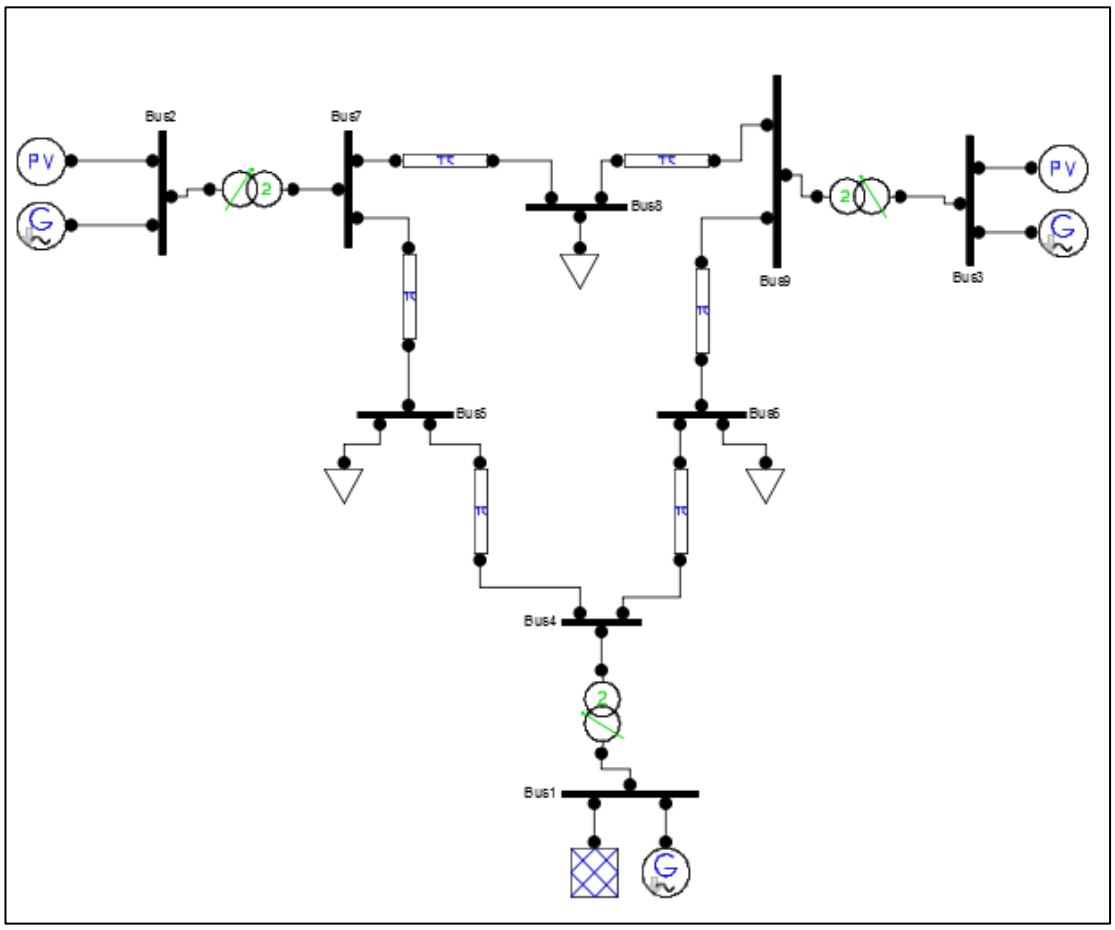

Reference: Made by O. B. Bekdikhan 2014

Table 9.1: Power flow results of IEEE 9-bus test system in PSAT

Bus Number	Voltage (pu)	Phase (deg)	P gen (pu)	Q gen (pu)	P load (pu)	Q load (pu)
1	1.04	0	0.71641	0.27046	0	0
2	1.025	9.28	1.63	0.06654	0	0
3	1.025	4.6648	0.85	-0.1086	0	0
4	1.0258	-2.2168	0	0	0	0
5	0.99563	-3.9888	0	0	1.25	0.5
6	1.0127	-3.6874	0	0	0.9	0.3
7	1.0258	3.7197	0	0	0	0
8	1.0159	0.72754	0	0	1	0.35
9	1.0324	1.9667	0	0	0	0

Reference: Made by O. B. Bekdikhan 2014

9.2 CONTINUATION POWER FLOW ANALYSIS OF IEEE 9-BUS TEST SYSTEM IN PSAT

After the power flow analysis, continuation power flow method was applied to test system. In first case, original IEEE 9 bus test system is used. Then, synchronous generator which is connected to bus 2 was changed with a DFIG and maximum loadability was found. CPF curves of these conditions can be seen in figure 9.3. In the original system loading parameter λ was calculated as 1.6219. However, when a synchronous generator is changed with a DFIG, this value decreases to 1.1069. Parameters of DFIG are included in Appendix E.

Figure 9.3: (a) CPF curve of original IEEE 9 bus test system (b) CPF curve of IEEE 9 bus test system with a DFIG

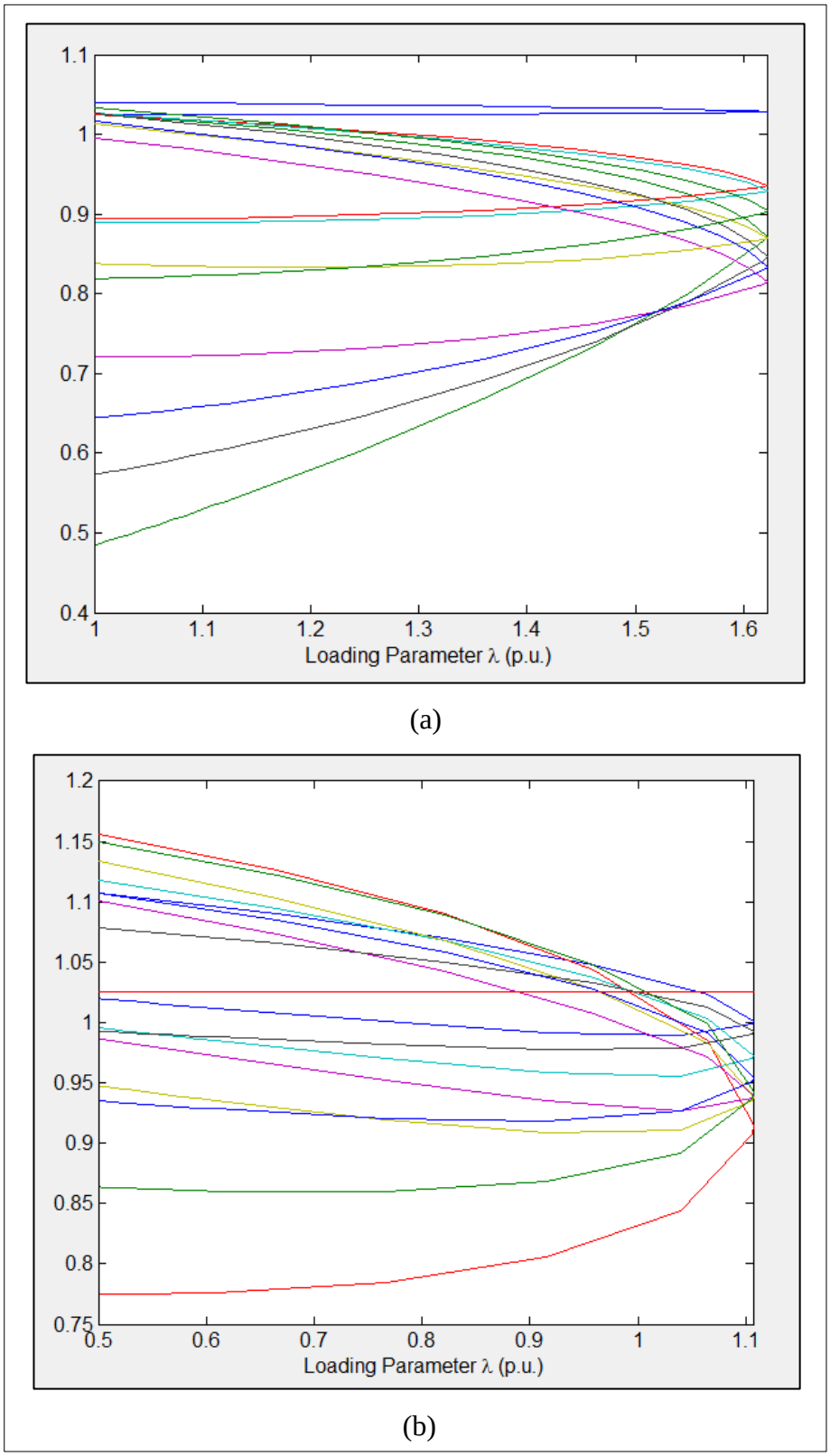

Reference: Made by O. B. Bekdikhan

10. CASE STUDY: TRAKYA TRANSMISSION SYSTEM

After the test system application, voltage stability effects of wind farms in Turkish electrical system can be investigated. Results of the interview with the "Trakya Load Dispatching Center", some part of Trakya region is chosen as case study and data of the region are obtained. The system consists of 5 generators, 25 buses (9 of them is 154 kV) and 9 transmission lines. In the original system, all of the generators are synchronous. There are no wind farms. The purpose of this thesis is comparison voltage stability effects of wind farms and conventional power plants. Therefore, a plant in the system is changed with DFIG-based wind farm and several scenarios were created and static and dynamic analyses were achieved by PSAT. Electrical system configuration can be found in appendix. However, real bus names and part of the Trakya region were not explained because of the confidential issues.

Firstly, power flow is applied to the original system (without a wind farm connection). Buses which have highest load are detected. Power flow results of the system are included in Table 10.1.

Table 10.1: Power flow results of Trakya electricity system

Bus Number	Voltages (pu)	Phases (deg)	P gen (pu)	Q gen (pu)	P load (pu)	Q load (pu)
Bus 1	1.045	-18.8354	0.37023	21.6288	0	0
Bus 2	1.045	-17.9723	0.2902	0.42228	0	0
Bus 3	1.0401	-18.1599	0	0	0	0
Bus 4	1	0	12.9616	1.5804	0	0
Bus 5	1	-7.361	0.30054	7.1031	0	0
Bus 6	1.0214	-20.6167	0	0	0.62	0.03
Bus 7	1.0214	-20.6167	0	0	0.62	0.03
Bus 8	1.0209	-20.9383	0	0	0.63	0.03
Bus 9	0.98207	-16.8171	0	0	0.63	0.01
Bus 10	0.98098	-18.0672	0	0	0.98	0.1
Bus 11	0.83786	-13.3466	0	0	0.7	0.07
Bus 12	0.84091	-11.7169	0	0	0.35	0.04
Bus 13	0.84126	-14.5992	0	0	0.92	0
Bus 14	1.0232	-19.0143	0	0	0.02	0
Bus 15	1.0188	-21.1924	0	0	0.54	0.02
Bus 16	1.0188	-21.1924	0	0	0.54	0.02
HV 1	0.84374	-10.2103	0	0	2.746	0.363
HV 2	0.99411	-3.8445	0	0	0	0
HV 3	1.0339	-7.388	0	0	0	0
HV 4	0.98896	-14.5763	0	0	1.85	0.54
HV 5	1.0232	-18.896	0	0	0	0
HV 6	1.0234	-18.805	0	0	0	0
HV 7	1.0203	-19.5067	0	0	1.34	0.197
HV 8	1.0287	-18.8509	0	0	0	0
HV 9	1.0235	-18.803	0	0	0	0

Reference: Made by O. B. Bekdikhan 2014

Then, in order to compare effects of wind farms and conventional plants and observe effects of wind farm, three case scenarios are created;

Case A:

Original Trakya transmission system was used. This system doesn't include any wind farm. Model of it can be seen in Appendix A.

Case B:

One of the conventional power plants in Trakya electricity system was changed with a DFIG-based wind farm. This farm has same power with the changing conventional power plant. Model of case B can be seen in the Appendix B.

Case C:

In original system, new wind farm was connected in the weakest bus. After new power plant installation, system configurations can be found in the Appendix C.

Simple machine model is used in all scenarios. After scenarios are created, following procedures are applied.

10.1 STATIC VOLTAGE STABILITY ANALYSIS OF TRAKYA TRANSMISSION SYSTEM WITH CONTINUATION POWER FLOW TECHNIQUE

In order to assess static voltage stability, continuation power flow method is applied to all cases in PSAT. CPF curves of all cases were drawn and maximum loadability limit was found. Effect of a DFIG based wind farm on loadability was detected. Data of DFIG and wind model is given in Appendix E.

Case A:

Firstly, original Trakya electricity system was used under normal operation condition. Table 2 shows power flow results of the system. According to that, 3 buses were selected for drawing CPF curve. As it can be clearly seen, bus 11 is the weakest bus for voltage. Also, HV 1 bus has the highest load. According to the results, bus 1 is the strongest bus. Therefore, these buses were especially selected for CPF curve. In the figure 10.1, CPF curve and maximum loadability limit can be seen.

Figure 10.1: CPF curve of Case A

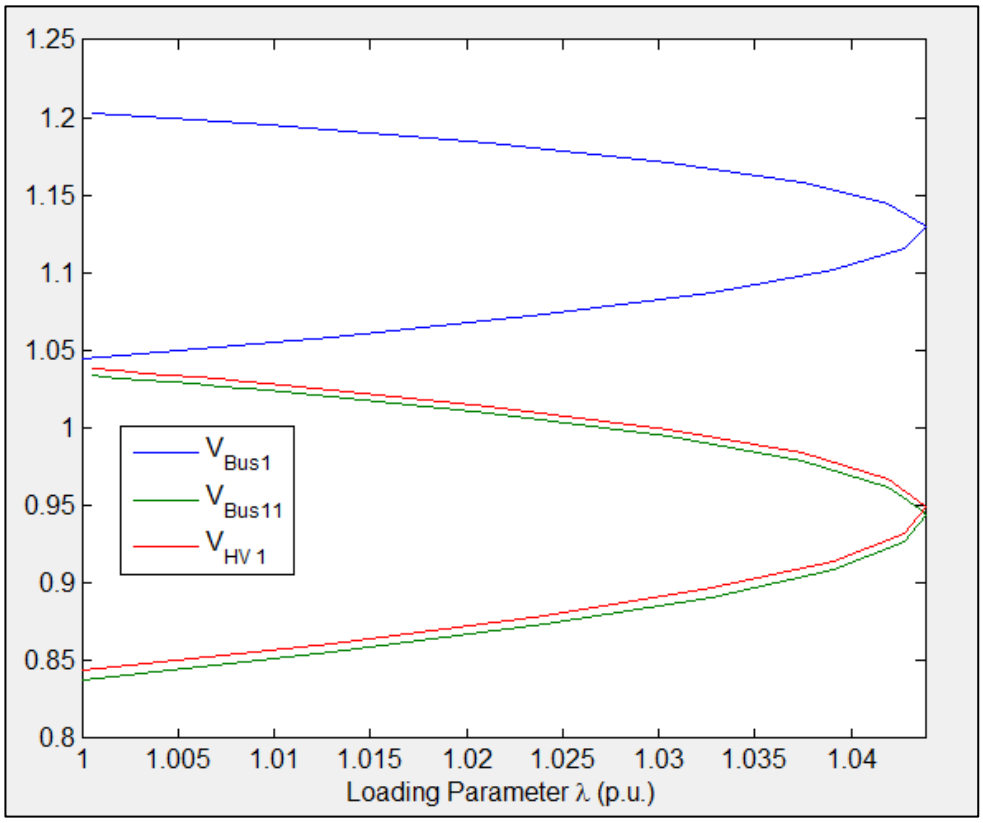

Reference: Made by O. B. Bekdikhan 2014

Case B:

In Case B, a conventional power plant was changed with a DFIG based wind farm. Wind farm has same power with the conventional plant. For this case, again continuation power flow method was applied. Maximum loadability limit of the new system was found. It was illustrated in figure 10.2. As it can be seen, loadability limit of the system decrease. In this case loading parameter λestimated as 1.025. It is 0.015 lower than case A.

Figure 10.2: CPF curve of Case B

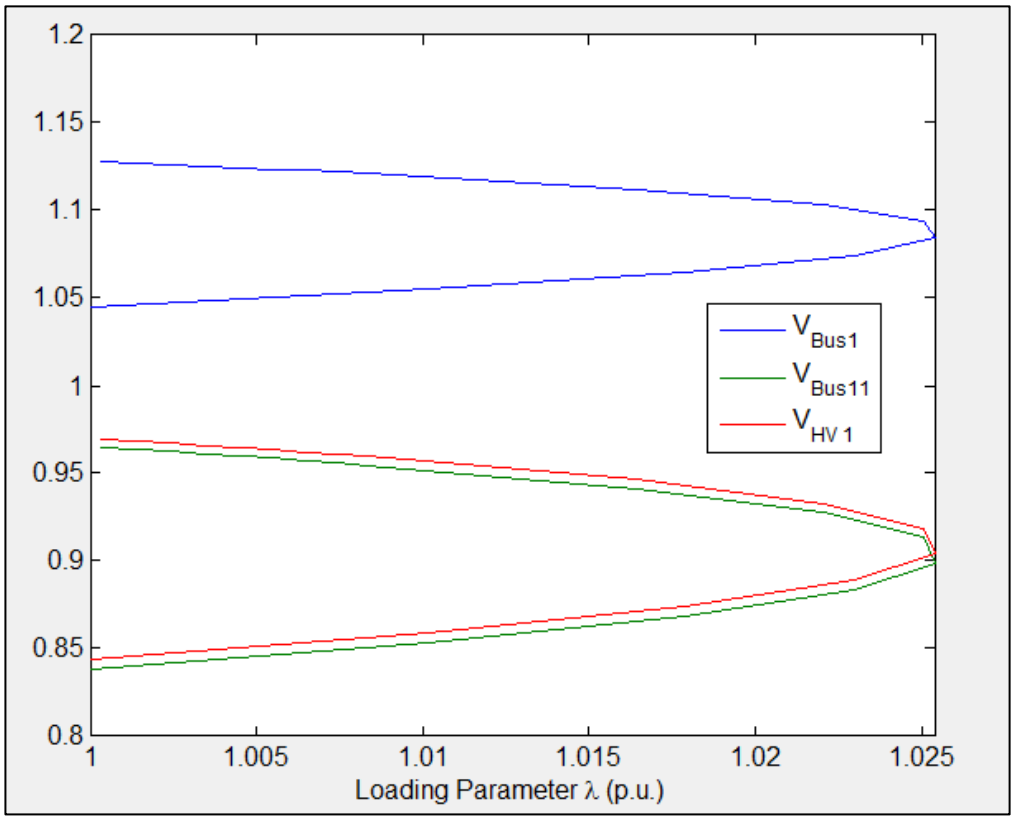

Reference: Made by O. B. Bekdikhan 2014

Case C:

Case C is similar to Case A. Only difference is an additional wind farm. In this case, at bus HV 2, again a DFIG based wind farm is connected. This farm is defined as PV generation bus. After the modelling, continuation power flow was applied and maximum loadability limit was found. Maximum loading parameter of case C is 1.318. As expected, a new farm's installation increases the system loadability because of increasing in electricity generation. Thus, highest loadability limit is obtained from case C. CPF curve is illustrated in figure 10.3.

Figure 10.3: CPF curve of Case C

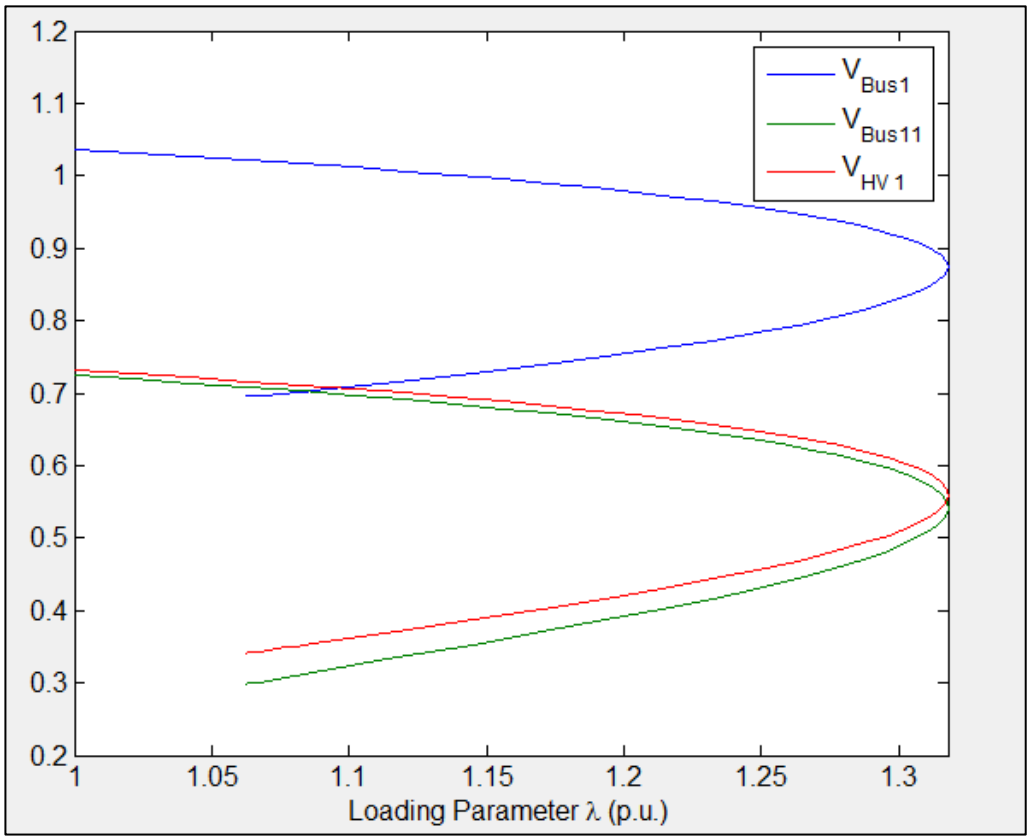

Reference: Made by O. B. Bekdikhan 2014

Consequently, static voltage stability analysis of Trakya electricity system was achieved. When a wind farm is connected instead of a conventional power plant, DFIG based wind farm decreased system maximum loadability limit. The reason of this decrement is machine type. As mentioned in section 6, bus voltage angles and cos θ of the machine are included in the mathematical model. These parameters affect system's loadability. DFIG's value of the cos θ is lower than the synchronous machine. Therefore, decrement in the loadability is an expected result. Also, effect of an additional wind farm installation is examined. When a wind farm is added to the original Trakya system, maximum loadability limit is increased.

10.2 DYNAMIC VOLTAGE STABILITY ANALYSIS OF TRAKYA TRANSMISSION SYSTEM WITH TIME DOMAIN SIMULATIONS

Fault Right-Through (FRT) is an important feature for the power systems. If system has high FRT capability, system can stay stable easier in terms of voltage. In order to understand behavior of the system after a fault occurrence, time domain simulations are applied. In time domain simulations, lots of different mathematical integration methods can be used. However, in this thesis, trapezoidal rule is preferred. In order to observe FRT contribution of the DFIG based wind farm and compare it with conventional power plants, time domain simulation were applied to Case A and Case B. a 3 phase fault is applied to the system and then it is cleared. After fault clearance, system was examined in terms of voltage.

Case A:

In original Trakya system, a three phase fault is occurred in bus 8 at 0.5 s and then it is cleared at 0.7s. In order to examine system behavior after the fault, time domain simulation was achieved. Voltage profile of the weakest bus (bus 11) and bus HV 1 which has highest load were examined. Voltage profile of the system can be observed in figure 10.4.

Figure 10.4: Voltage profile after a fault occurrence for Case A

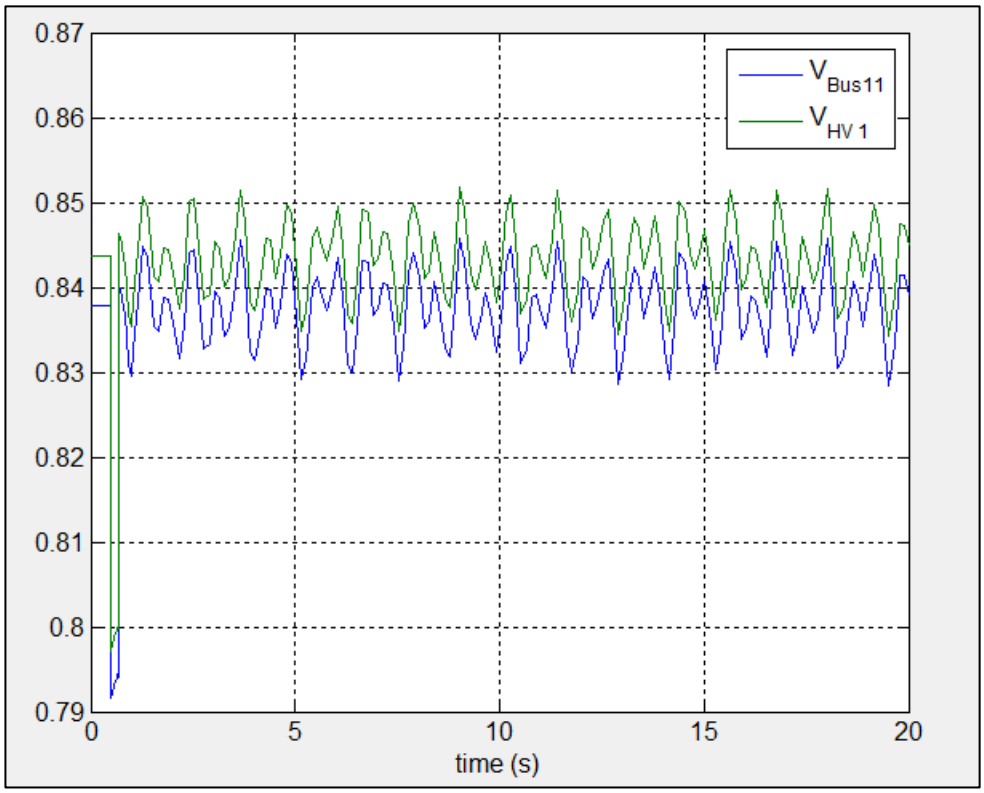

Reference: Made by O. B. Bekdikhan 2014

Case B:

In order to examine behavior of a wind farm after a fault occurrence, time domain simulation was completed for Case B. Again same three phase fault was applied to bus 8 and then it was cleared. Voltage profiles of bus 11 and bus HV1 were illustrated in figure 10.5. As it can be clearly seen, wind farm connection contributes to dynamic behavior of the power system. It damps oscillation of voltages when compares with a conventional plant. In Case A, voltage oscillations after the fault is between 0.83 and 0.845 pu for bus 11 and for bus HV 1, voltage is between 0.835 and little above 0.85 pu. However, this rate is lower in Case B. Voltage oscillations of bus 11 is between 0.835 and 0.845 and for bus HV 1 oscillation is between approximately 0.84 and 0.85. Also, in case B, oscillations are more smoothless than Case A. Consequently, wind farm connection contributes to system fault ride through capability.

Figure 10.5: Voltage profile of Case B after a fault occurrence

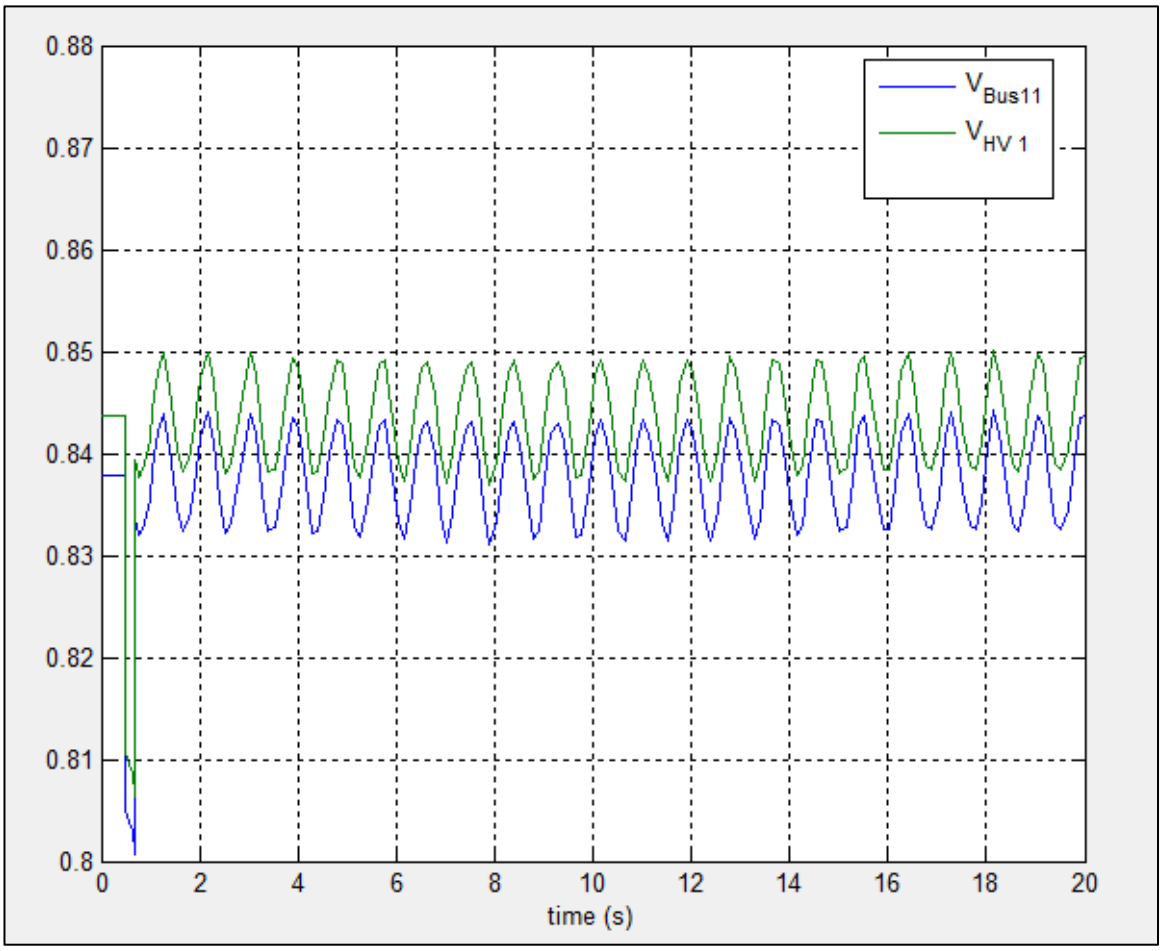

Reference: Made by O. B. Bekdikhan 2014

10.3 FACTS DEVICES EFFECTS ON TRAKYA TRANSMISSION SYSTEM

As mentioned in the literature survey, reactive power compensation is an important factor for voltage stability. Lots of FACTS devices are used nowadays. In order to investigate effects of FACTS devices, these devices were connected to weakest bus and time domain simulation was completed for Case A and Case B. Then system's situation was found after a fault occurrence in terms of voltage. Firstly, 100 MVA STATCOM is connected to bus 11 and simulations were done. In figure 10.6, STATCOM's effect in Case A can be seen.

Figure 10.6: (a) Voltages at bus 11 and bus HV 1 for Case A

(b) Voltages at bus 11 and bus HV 1 when 100 MVA STATCOM is connected to bus 11 for Case A

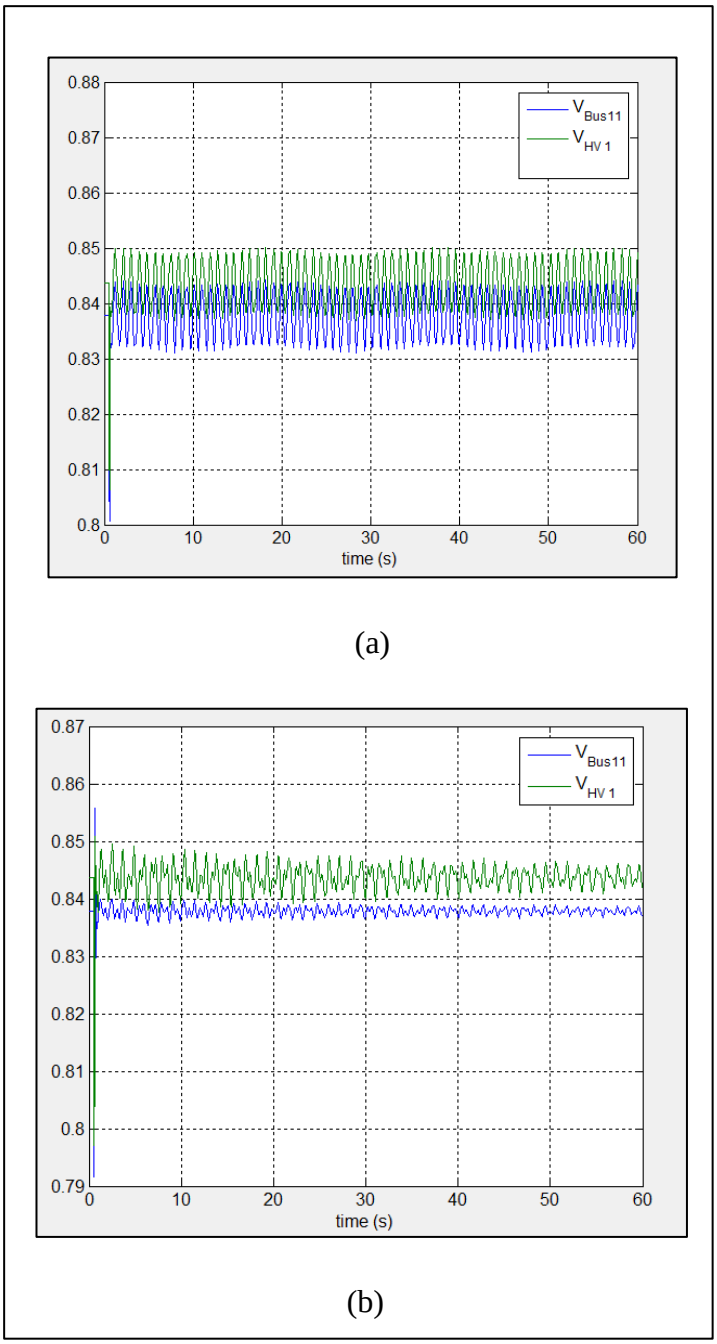

Reference: Made by O. B. Bekdikhan 2014

From figure 10.6, it can be clearly seen that STATCOM contributes to voltage stability. STATCOM is just connected to bus 11. However, it not only corrects voltage of bus 11 but also correct voltage of bus HV 1.

When all process is applied for Case B, again STATCOM contributes to voltage stability. It can be seen from figure 10.7.

Figure 10.7: (a) Voltages at bus 11 and bus HV 1 for Case B (b) Voltages at bus 11 and bus HV 1 when 100 MVA STATCOM is connected to bus 11 for Case B

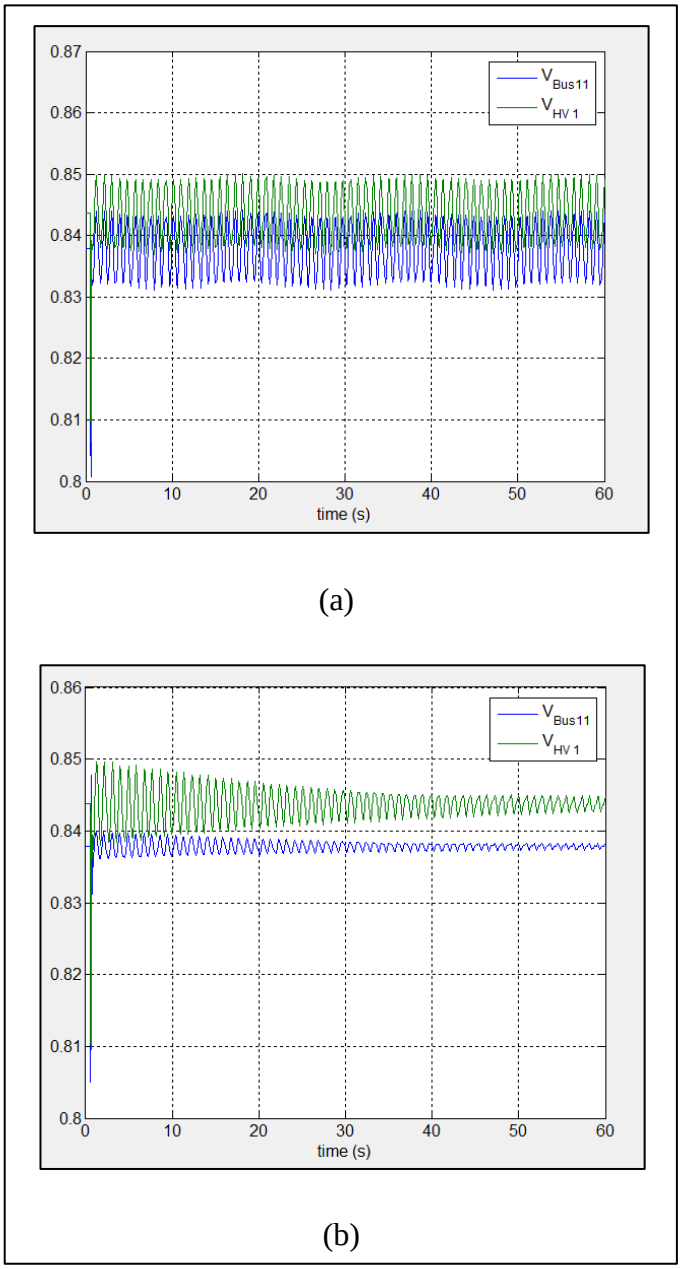

Reference: Made by O. B. Bekdikhan 2014

From figure 10.7, it can clearly be seen that STATCOM contributes to correct voltages at both buses. When STATCOM connection compares with Case A, it gives better solution with wind farm connection. Wind farm increase system transient stability and it

prevent voltage collapse. The difference between a conventional power plant and a DFIG based wind farm can be observed easily in figure 10.8.

Figure 10.8: (a) STATCOM connection for Case B
(b) STATCOM connection for Case B

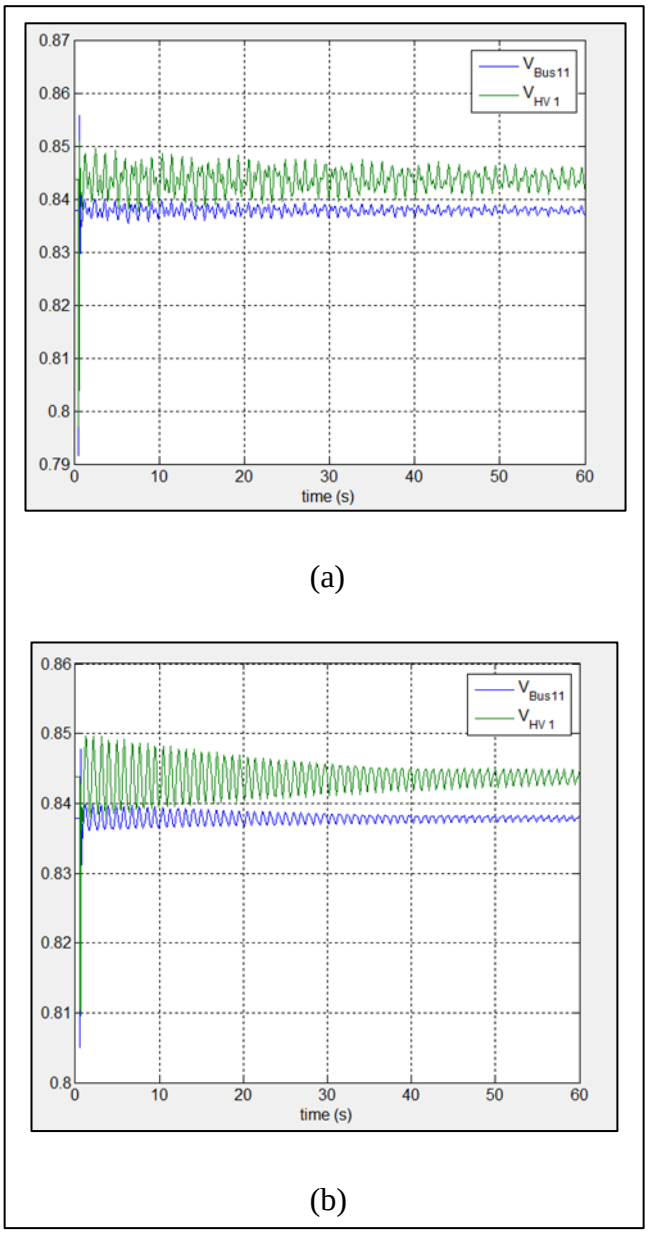

Reference: Made by O. B. Bekdikhan 2014

Same process was achieved for 100 MVA SVC connection instead of STATCOM. Firstly, for Case A, 100 MVA SVC was connected at bus 11. Then, effects of SVC were compared with STATCOM performance in figure 10.9. As it can clearly be seen,

STATCOM more effective then SVC for providing voltage stability. Voltage oscillations lower with STATCOM connection when it compares with SVC usage.

Figure 10.9: (a) 100 MVA STATCOM connection for Case A
(b) 100 MVA SVC connection for Case A

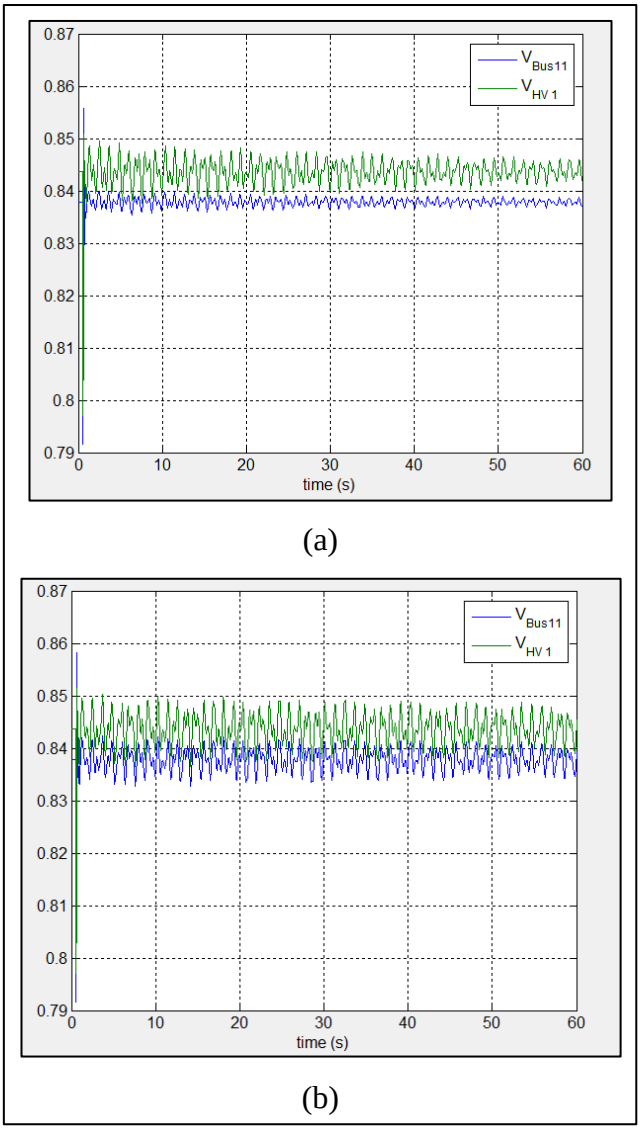

Reference: Made by O. B. Bekdikhan

Comparison of STATCOM and SVC was achieved for the Case B. Results are represented in Figure 10.10. Again STATCOM shows better results.

Figure 10.10: (a) 100 MVA STATCOM connection for Case B
(b) 100 MVA SVC connection for Case B

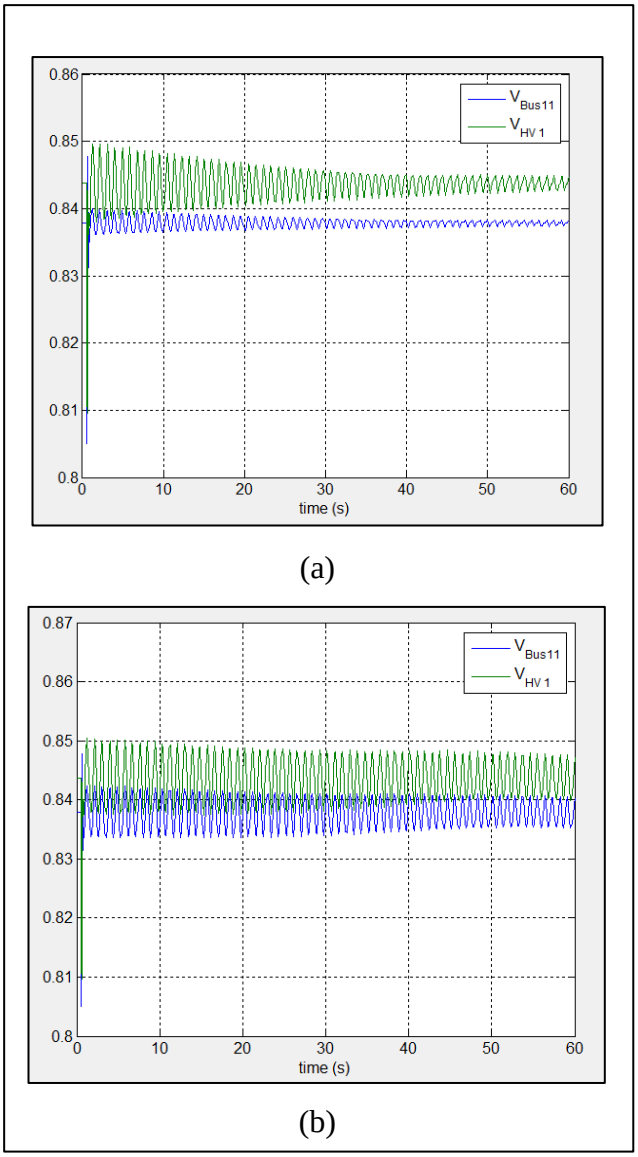

Reference: Made by O. B. Bekdikhan

After the STATCOM and SVC comparison, UPFC's effect was investigated. 100 MVA UPFC with a constant voltage operation mode was connected to the transmission line between HV1 and HV2. Then, time domain simulations were achieved for both cases and results were compared with STATCOM performance. In figure 10.11, comparison for Case A can be seen.

Figure 10.11: (a) 100 MVA STATCOM connection for Case A
(b) 100 MVA UPFC connection for Case A

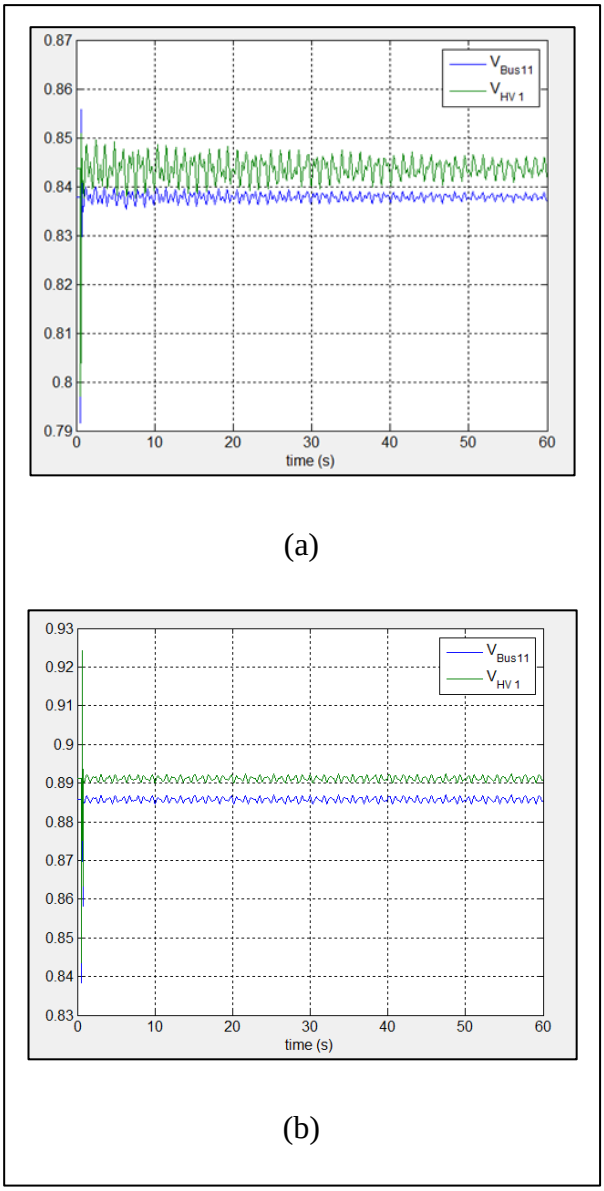

Reference: Made by O. B. Bekdikhan 2014

When fault is occurred, voltages decrease in all cases. However, in UPFC connection, voltage dip is less than the STATCOM connection case. Also, voltage oscillations are rather small when it compare with STATCOM connection case. Consequently, UPFC gives best results for supplying voltage stability. With UPFC usage, voltage oscillations are more damped after a fault occurrence.

Same process was applied for Case B too. Results can be observed in figure 10.12.

Figure 10.12: (a) 100 MVA STATCOM connection for Case B
(b) 100 MVA UPFC connection for Case B

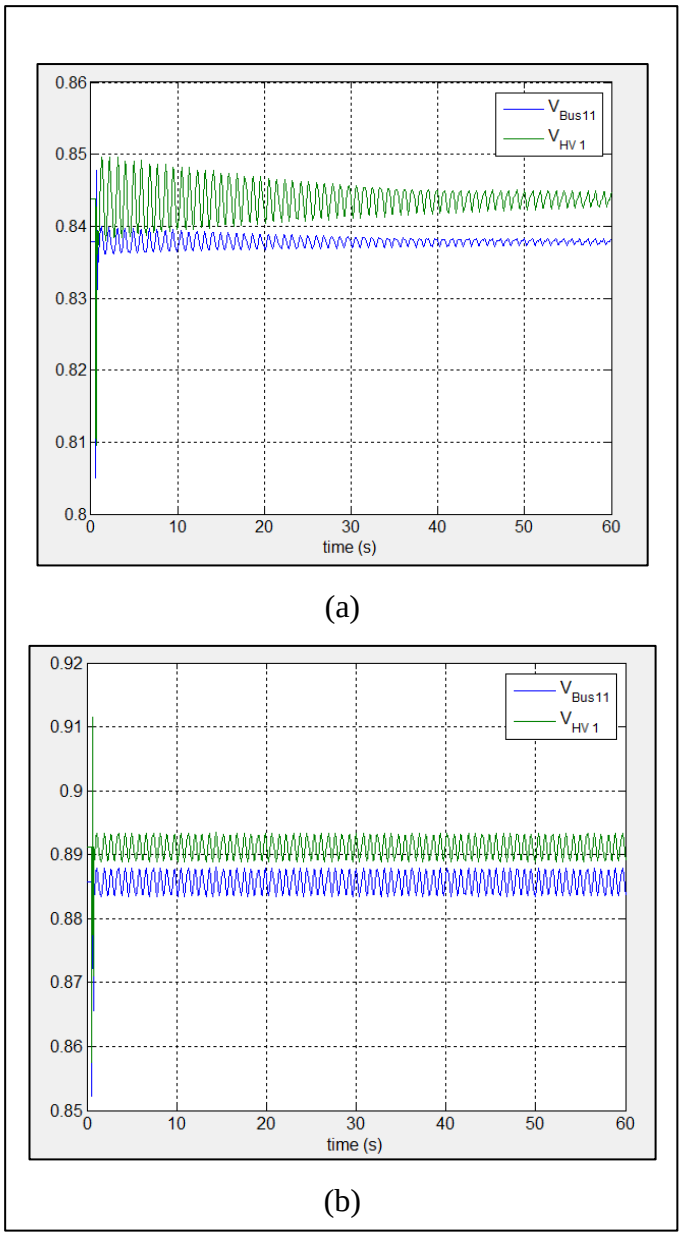

Reference: Made by O. B. Bekdikhan 2014

11. CONCLUSION

Increasing in renewable energy usage causes lots of voltage stability problems. The most important one is voltage stability problems. In this thesis, grid connection of wind energy which is most popular renewable energy source was examined. Firstly, a literature review was achieved and deficiencies were detected. Then, solutions for supplying voltage stability were investigated. Continuation power flow method was explained to complete static voltage stability analysis. Then, time domain simulation method was investigated for making dynamic voltage stability analysis. In addition, reactive power compensation methods especially FACTS devices were investigated for supporting voltage stability. After these, in order to observe grid connection effect of wind farms on a real system, Trakya Transmission System was selected as a case study. Also, PSAT which is a MATLAB toolbox was chosen as simulation program. However, in order to prove reliability of PSAT, firstly power flow was completed for IEEE 9 bus test system and results were compared. True results were obtained. After reliability test, continuation power flow was applied original IEEE system. Then, a conventional plant in the system was changed with a DFIG based wind farm and again CPF was applied. As expected, maximum loadability limit decreased when a plant is changed with wind farm because of the machine type.

After the IEEE 9 bus test system, real case study Trakya Transmission System was simulated in PSAT. Data of the region were obtained from Trakya Load Dispatching Center. After the system simulation, voltage stability analyzes were achieved for different scenarios.

In first scenario, original Trakya Transmission System was used. In the original system, there is no wind farm installation. This system includes 5 synchronous generators, 25 buses (9 of them is 154 kV) and 9 transmission lines. For the static analysis, continuation power flow method was applied to the original system and maximum loadability was found as 1.0439.

In order to observe wind farm's voltage stability effect, a conventional plant of the system was changed with a DFIG based wind farm in second scenario. This wind farm has same power with the conventional power plant. Thus, comparison of wind farms

and conventional power plants were achieved. After the continuation power flow application, it was found that maximum loadability decrease to 1.0254. As mentioned, same situation observed in IEEE test case.

After the static voltage stability analysis, dynamic analysis was applied for both cases. Fault ride through capability of wind farm and conventional power plants were compared. Firstly, weakest and high loaded buses of the original system were detected with power flow. The weakest bus in terms of voltage is bus 11. Also, it was found that bus HV1 has highest load. Therefore, dynamic analysis results were observed on these buses. A three phase fault was applied at 0.5s and then it was cleared at 0.7s. Then comparison of DFIG based wind farm and a conventional power plant was achieved in terms of voltage. When the results of two cases were compared, it was found that wind farm more contributes to damping voltage oscillations.

Also, effects of FACTS devices which becomes popular last decades were investigated. Three different FACTS devices were selected. These are STATCOM, SVC and UPFC. All of them were connected to weakest bus for both cases. It was founded that FACTS usage with a wind farm gives better results for voltage stability. In addition, these three devices were compared with each other. The best results were obtained respectively with UPFC, STATCOM and SVC.

In conclusion, wind farms cause decrement in maximum loadability of the system. However, in fault conditions, they more effective than the conventional power plants. Wind farms increase the fault ride through capacity of the system. Thus, they are more effective to remain voltage stable of the system and prevent voltage collapse.

In future works;

i. Not only DFIG based wind farms but also effects of SCIG and synchronous generator based wind farms can be examined.
ii. Harmonic analysis for wind farm connection can be investigated.
iii. More than one FACTS usage effect and effects of FACTS's optimal location can be examined.
iv. Dynamic analysis is not done in Load Dispatching Centers. Therefore, another region can be selected.

v. Also, voltage stability effects of other renewable sources especially solar energy can be investigated.

vi. Maximum wind power capacity which can connect to the grid can be investigated.

REFERENCES

Books

Kundur, P., 1994. *Power system stability and control*. New York: MCGraw-Hill.

Padiyar, K.R., 2004. *Power system dynamics stability and control*. Second Edition. India: B.S. Publications.

Sauer, P.W. and Pai, M.A., 1998. *Power system dynamics and stability*. New Jersey: Prentice-Hall.

Tacer, M.E., 1990. *Enerji sistemlerinde kararlılık*. İstanbul: İTÜ.

Periodicals

Ajjarapu, V. and Christy, C., 1992. The continuation power flow: a tool for steady state voltage stability analysis. *IEEE Transactions on Power Systems*. **7** (1) pp. 416 – 423

Bhumkittipich, K., Jan-Ngurn, C., 2013. Study of voltage stability for 22kv power system connected with lamtakhong wind power plant, Thailand. *Energy Procedia*. **34**, pp.951-963.

Chiang, H-D., Flueck, A.J., Shah, K.S., Balu, N., 1995. Cpflow: a practical tool for tracing power system steady-state stationary behavior due to load and generation variations. *IEEE Transactions on Power Systems*. **10** (2) pp. 623-635.

Khattara, A., Bahri, M., Aboubou, A., Becherif, M., Ayad, M.Y., 2013. Line-fault ride-through (lfrt) capabilities of dfig wind turbine connected to the power system. *APCBEE Procedia*. **7**, pp. 189 – 194.

Li, H. and Chen, Z., 2008. Overview of different wind generator systems and their comparisons. *IET Renewable Power Generation*. **2** (2), pp. 123-138

Luna, A., Lima, F.K.A., Santos, D., Rodriguez, P., Watanabe, E.H., Arnaltes, S., 2011. Simplified modeling of a dfig for transient studies in wind power applications. *IEEE Transactions on Industrial Electronics*. **58** (1), pp. 9-20.

Shafiullah, G.M., Amanullah M.T.Oo., Shawkat A.B.M, Wolfs P., 2013. Potential challenges of integrating large-scale wind energy into the power grid–A review. *Renewable and Sustainable Energy Reviews*. **20**, pp. 306-321.

Others

Abdelhalim, H.M., Farid, A.M., Adegbege, A.A., Youcef-Toumi, K., 2013. Transient stability of power systems with different configurations for wind power integration. *Innovative Smart Grid Technologies (ISGT)*. 24-27 Feb. 2013 Washington, DC, pp. 1-7.

Aly, M.M and Abdel-Akher, M., 2011. Voltage stability assessment for radial distribution power system with wind power penetration. *IET Conference on Renewable Power Generation (RPG 2011)*. 6-8 Sept. 2011 Edinburgh, pp. 1 – 6.

Camm, E.H., Behnke, M.R., Bolado, O., Bollen, M., Bradt, M., Brooks, C., Dilling, W., Edds, M., Hejdak, W.J., Houseman, D., Klein, S., Li, F., Li, J., Maibach, P., Nicolai, T., Patino, J., Pasupulati, S.V., Samaan, N., Saylors, S., Siebert, T., Smith, T., Starke, M., Walling, R., 2009. Characteristics of wind turbine generators for wind power plants. *Power & Energy Society General Meeting*. 26-30 July 2009 Calgary, AB, IEEE, pp. 1-5.

Canizares, C.A., 1991. Voltage collapse and transient energy function analyses of ac/dc systems, University of Wisconsin, https://ece.uwaterloo.ca/~ccanizar/papers/phd.pdf [accessed 15 March 2014].

Canizares, C.A., 2000. Power flow and transient stability models of FACTS controllers for voltage and angle stability studies. *IEEE Power Engineering Society Winter Meeting*. 23-27 Jan 2000, pp. 1447 – 1454

Chen, Z., 2005. Issues of connecting wind farms into power systems. IEEE/PES *Transmission and Distribution Conference & Exhibition: Asia & Pacific*. Dalian-China, pp. 1-6.

Ertay, M.M. and Aydoğmuş, Z., 2011. Güç sistemlerinde FACTS uygulamaları. *6th International Advanced Technologies Symposium*. 16-18 May 2011, pp. 370-376.

Garcia, D., Luis, J., 2009. Modeling and control of squirrel cage induction generator with full power converter applied to windmills, University of Oulu, http://upcommons.upc.edu/pfc/bitstream/2099.1/10692/1/SCIG%20with%20Full%20Power%20Converter_book2sides.pdf [accessed 10 January 2014]

Güleryüz, M., (2010). FACTS cihazları ve rüzgar enerji santrallerinin gerilim kararlılığına etkilerinin incelenmesi. *Thesis for the M.A. Degree*. İstanbul: İTÜ.

Hasani, M., Parniani, M., 2005. Method of combined static and dynamic analysis of voltage collapse in voltage stability assessment. *IEEE/PES Transmission and Distribution Conference & Exhibition: Asia & Pacific*. Dalian-China, pp. 1-6.

Jimoh, A.A., Venter, P-J., Appiah, E.K., 2012, Modelling and analysis of squirrel cage induction motor with leading reactive power injection, Tshwane University of Technology, http://www.intechopen.com/books/induction-motors-modelling-and-control/modelling-and-analysis-of-squirrel-cage-induction-motor-with-leading-reactive-power-injection [accessed 10 January 2014].

Jing, X., 2009, Modeling and control of a doubly-fed induction generator for wind turbine-generator systems, Marquette University, http://epublications.marquette.edu/cgi/viewcontent.cgi?article=1166&context=theses_open [accessed 5 December 2013].

Kamarposhti, M.A., Alinezhad, M., Lesani, H., Talebi, N., 2008. Comparison of SVC, STATCOM, TCSC, and UPFC Controllers for Static Voltage Stability Evaluated by Continuation Power Flow Method. *Electric Power Conference*. 6-7 Oct. 2008 Vancouver, pp. 1-8.

Keskin, M.B., 2007. Continuation power flow and voltage stability in power systems, ODTÜ, http://etd.lib.metu.edu.tr/upload/12608718/index.pdf [accessed 20 April 2014].

Munoz, J.C. and Canizares, C.A., 2011. Comparative stability analysis of DFIG-based wind farms and conventional synchronous generators. *Power Systems Conference and Exposition (PSCE)*. 20-23 March 2011 Phoenix, AZ, pp. 1-7.

Ofualagba, G. and Ubeku, E.U., 2008. Wind energy conversion system- wind turbine modeling. *Power and Energy Society General Meeting - Conversion and Delivery of Electrical Energy in the 21st Century*. 20-24 July 2008 Pittsburgh, PA, pp. 1-8.

Pierik, J.T.G., Morren, J., Wiggelinkhuizen, E.J., De Haan, S.W.H., Van Engelen, T.G., Bozelie, J., 2004. Electrical and control aspects of offshore wind farms II (Erao II), Delft University of Technology, http://www.ecn.nl/docs/library/report/2004/c04050.pdf [accessed 20 August 2013]

Polinder, H., Van der Pijl, F.F.A., De Vilder, G.-J., Tavner, P., 2005. Comparison of direct-drive and geared generator concepts for wind turbines. *IEEE Electric Machines and Drives Conference*. 15-15 May 2005 San Antonio, TX, pp. 543 – 550.

TUREB, 2014. *Türkiye Rüzgar Enerjisi İstatistik Raporu*. Temmuz. İstanbul.

Xiaodong, Y., Zhi, W., Qun, L., Jiankun, L., Jingbo, Z., Wei, G., 2010. Simulation and analysis of wind farm reactive power and voltage problems based on detailed

model. *2010 China International Conference on Electricity Distribution (CICED)*. 13-16 Sept. 2010 Nanjing, pp. 1-7.

Zeng, Z., Li, X., Zhou, J., Zhang, Y., 2009. Investigation of wind farm on power system voltage stability based on bifurcation theory. *Asia-Pacific Power and Energy Engineering Conference*. 27-31 March 2009 Wuhan, pp. 1 – 4.

APPENDICES

APPENDIX A

Original Trakya Electricity System model in PSAT:

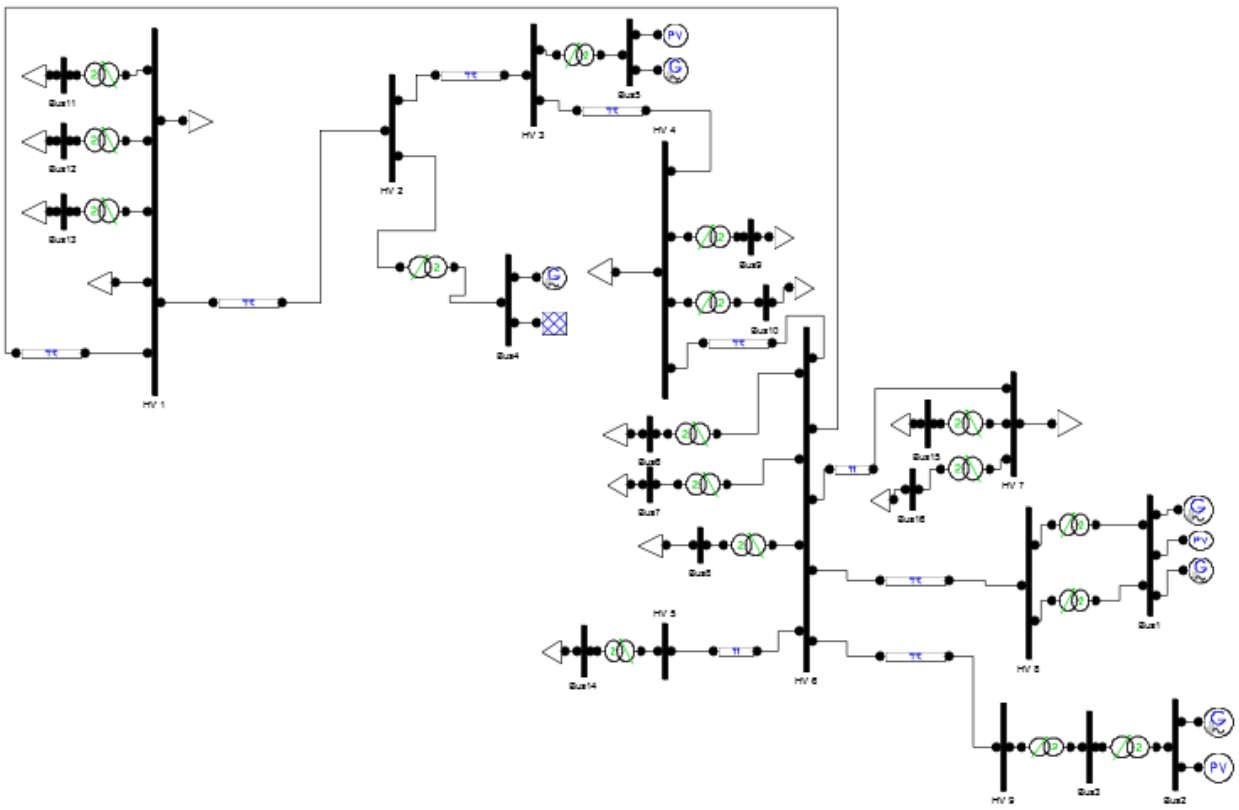

APPENDIX B

Model of Trakya Electricity System with a wind farm connection:

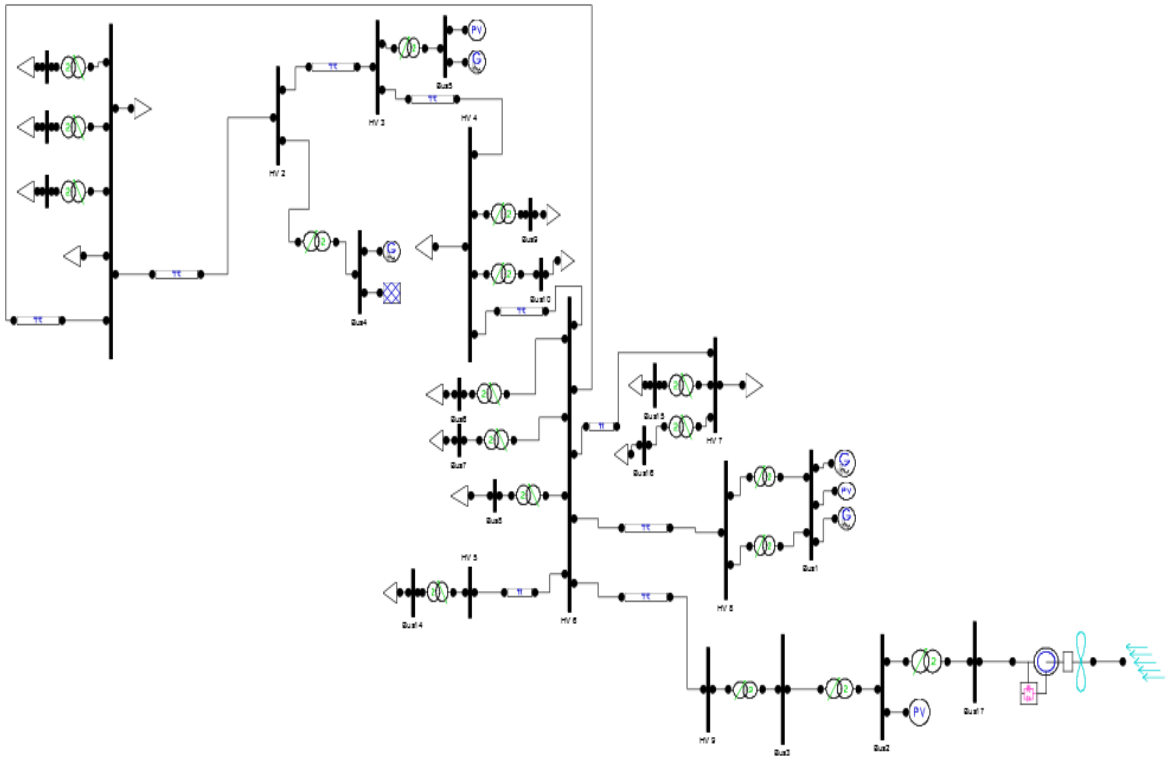

APPENDIX C

Model of Trakya Electricity System with an additional wind farm connection

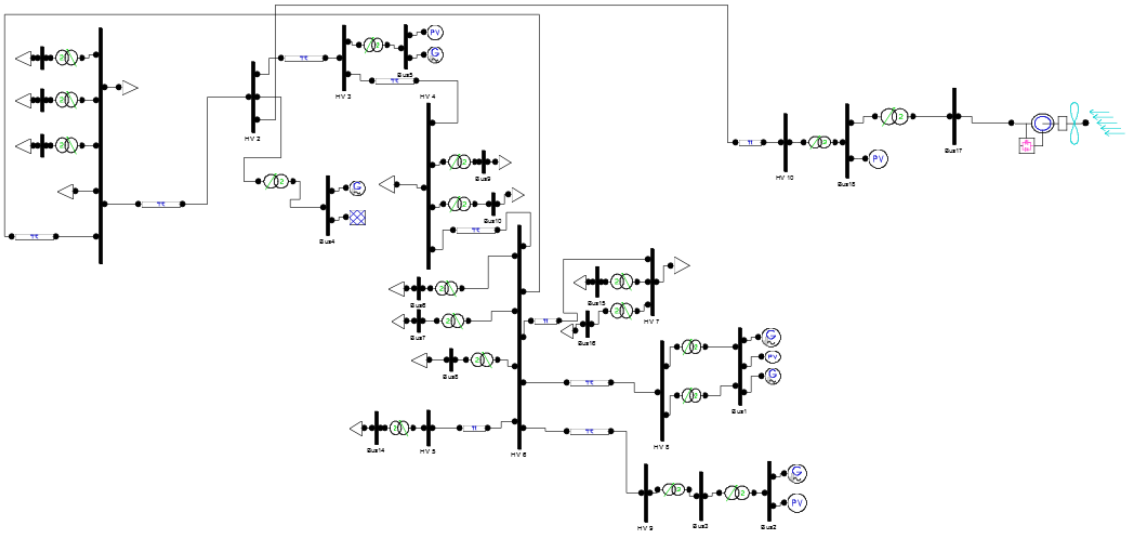

APPENDIX D

Data of IEEE 9 bus test system

Line	Base Power (MVA)	Voltage (kV)	Frequency (Hz)	Resistance (pu)	Reactance (pu)	Susceptance (pu)
9-8	100	230	60	0.0119	0.1008	0.209
7-8	100	230	60	0.0085	0.072	0.149
9-6	100	230	60	0.039	0.17	0.358
7-5	100	230	60	0.032	0.161	0.306
5-4	100	230	60	0.01	0.085	0.176
6-4	100	230	60	0.017	0.092	0.158
2-7	100	18	60	0	0.0625	0
3-9	100	13.8	60	0	0.0586	0
1-4	100	16.5	60	0	0.0576	0

Generator's data

Parameters	Generator 1	Generator 2	Generator 3
H (sec)	23.64	6.4	3.01
x_d (pu)	0.146	0.8958	1.3125
x'_d (pu)	0.0608	0.1198	0.1813
x_q (pu)	0.0969	0.8645	1.2578
x'_q (pu)	0.0969	0.1969	0.25
T'_{d0} (pu)	8.96	6.0	5.89
T'_{q0} (pu)	0.31	0.535	0.6

APPENDIX E

Parameters of DFIG, wind model and additional transformer (Munoz and Canizares 2011)

Wind model type	**Weibull Distribution**
Average wind speed (m/s)	14.50
Air density ρ ($^{kg}/_{m^3}$)	1.225
Filter time constant (s)	4
Sample time for wind measurements Δt (s)	0.1
Scale factor for Weibull distribution c	20
Shape factor for Weibull distribution k	2
Frequency step Δf (Hz)	0.2

Power Rating S_n (MVA)	63.5
Voltage Rating V_n (kV)	0.480
Frequency Rating f_n (Hz)	50
Stator Resistance R_s (pu)	0.01
Stator Reactance X_s (pu)	0.10
Rotor Resistance R_r (pu)	0.01
Rotor Reactance X_r (pu)	0.08
Magnetization Reactance X_m (pu)	3.00
Initial Constant H_m ($^{kWs}/_{kVA}$)	3.00
Pitch Control Gain K_p (pu)	10
Pitch Control Time Constant T_p (s)	3
Rotor Radius R (m)	75
Number of poles p	4
Number of blades	3
Gearbox Ratio	1/89
P_{max} (pu)	0.9
P_{min} (pu)	0.0
Q_{max} (pu)	0.35
Q_{min} (pu)	-0.219
Number of wind generators that compose to park	15

Data of additional transformer

Voltage Ratio (kV/kV)	0.480/11.5
Resistance (pu)	0
Reactance (pu)	0.1
Fixed Tap Ratio	1.00